Geochimica et Cosmochimica Acta Vol. 57, pp. 1817–1835

0016-7037/93/$6.00 + .00

Thermochronology of the Cornubian batholith in southwest England: Implications for pluton emplacement and protracted hydrothermal mineralization

J. T. CHESLEY,[1,*] A. N. HALLIDAY,[1] L. W. SNEE,[2] K. MEZGER,[1,3] T. J. SHEPHERD,[4] and R. C. SCRIVENER[5]

[1] Department of Geological Sciences, University of Michigan, Ann Arbor, MI 48109, USA
[2] USGS, Denver, CO 80225, USA
[3] Max-Plank-Institut für Chemie, Saarstrasse 23, D-6500 Mainz, Germany
[4] British Geological Survey, Keyworth, Nottingham NG12 5GG, UK
[5] British Geological Survey, Exeter EX4 6BX, UK

(*Received May* 25, 1992; *accepted in revised form October* 29, 1992)

Abstract—The metalliferous ore deposits of southwest England are associated with biotite-muscovite granites that intruded upper Paleozoic sediments and volcanic rocks at the end of the Hercynian Orogeny. The hydrothermal mineralization can be subdivided into four stages: (1) exoskarns; (2) high-temperature tin and tungsten oxide-bearing sheeted greisen bordered veins and Sn-bearing tourmaline veins and breccias; (3) polymetallic quartz-tourmaline-chlorite-sulfide-fluorite-bearing fissure veins, which represent the main episode of economic mineralization; and (4) late-stage, low-temperature polymetallic fluorite veins. U-Pb dating of monazite and xenotime and $^{40}Ar/^{39}Ar$ dating of muscovite were used to determine emplacement ages and cooling times for individual plutons within the Cornubian batholith, as well as separate intrusive phases within the plutons. In addition, $^{40}Ar/^{39}Ar$ ages from hornblende and secondary muscovite and Sm-Nd isochron ages from fluorite were employed to determine the relationship between pluton emplacement and different stages of mineralization. The U-Pb ages indicate that granite magmatism was protracted from ~300 Ma down to ~275 Ma with no evidence of a major hiatus. There is no systematic relation between the age of a pluton and its location within the batholith. The U-Pb ages for separate granite phases within a single pluton are resolvable and indicate that magma emplacement within individual plutons occurred over periods of as much as 4.5 myrs. Felsic porphyry dike emplacement was coeval with plutonism, but continued to ~270 Ma. The geochronologic data suggest that the Cornubian batholith originated from repeated melting events over 30 myrs and was formed by a series of small coalescing granitic bodies. Cooling rates of the main plutons are unrelated to emplacement age, but decrease from the southwest to the northeast from ~210°C myr^{-1} to ~60°C myr^{-1} with a mean of 100°C myr^{-1}. These slow cooling rates appear to reflect the addition of heat from multiple intrusive episodes. The mineralization history is distinct for each pluton and ranges from coeval with, to up to 40 myrs younger than the cooling age for the host pluton. Stage 2 mineralization is broadly synchronous with the emplacement of granite magmas, is dominated by fluids expelled during crystallization, and may be repeated by the emplacement of younger magmas within the same pluton. Sm-Nd isochrons for fluorite from stage 3 polymetallic mineralization give ages of 259 ± 7, 266 ± 3 and 267 ± 12 Ma, postdating stage 2 mineralization by up to 25 myrs within the same deposit. The similarity in age of the main polymetallic mineralization hosted by the oldest and youngest plutons, suggests that this stage of mineralization is unlikely to be related to hydrothermal circulation driven by the emplacement and cooling of the host granite. The mineralization is more likely the product of regional hydrothermal circulation driven by heat from the emplacement and crystallization of younger buried pulses of magma.

INTRODUCTION

PITCHER ET AL. (1985), defined a pluton as "a certain unity of structure characterizing magmas emplaced within a single, continuous outer contact: so defined plutons can have resulted from single or multiple injection." Many examples of plutons of a composite nature are available. Although there should be no genetic or chronologic connotation in the use of the term *pluton*, such implications are common in the literature. Modern high-precision geochronology may permit the direct resolution of the emplacement history of individual plutons. In addition, ages for the different stages of mineralization may be used in conjunction with the emplacement and cooling history of the batholith to elucidate the chronology of hydrothermal circulation associated with the deposition of major ore deposits.

The generally accepted model for granite-related hydrothermal mineralization assumes that pluton emplacement, hydrothermal circulation, and mineral deposition take place over a geologically insignificant period of time ($<10^6$ yr) (e.g., SKINNER, 1979; CATHLES, 1981, 1990; NESBITT, 1990). This conclusion is based on (a) quantitative models which suggest that in the presence of hydrothermal convection a pluton will cool in as little as 10^4 to 10^5 years (CATHLES, 1981, 1990; NORTON and KNIGHT, 1977; NORTON and TAYLOR, 1979); (b) the existence of porphyry copper deposits on Pacific islands that formed over one to two million years (SKINNER, 1979); (c) calculations of the lifetime of active geothermal systems (e.g., WHITE and HEROPOULOS, 1986); and (d) isotopic age determinations of host plutons and associated mineralization which have been unable to resolve differences in age (e.g., SKINNER, 1979; NORTON and

* *Present address:* Department of Geosciences, University of Arizona, Tucson, AZ 85721, USA.

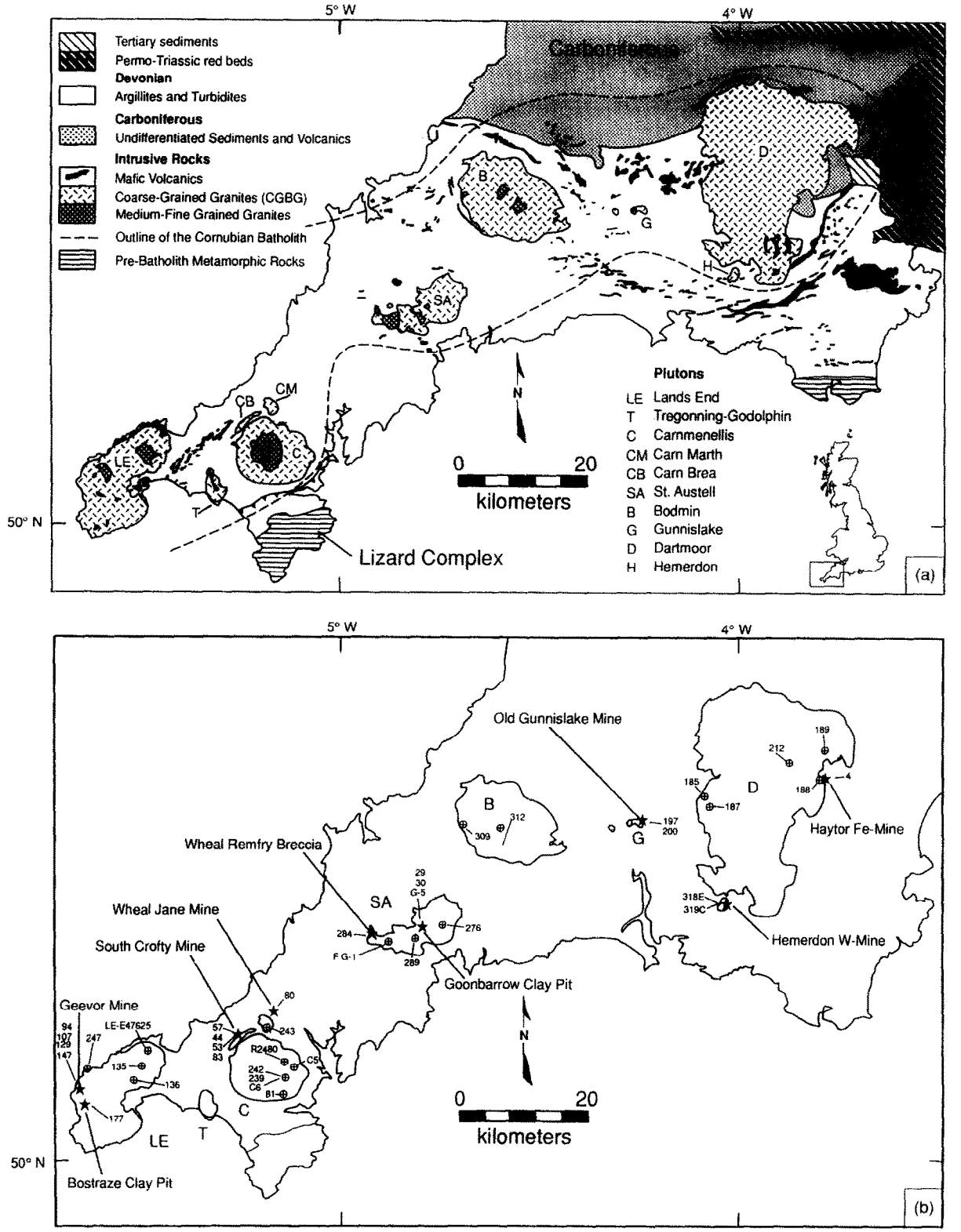

FIG. 1. (a) Generalized geologic map of the Cornubian batholith in southwest England, modified from EDMONDS et al. (1969) and WILLIS-RICHARDS and JACKSON (1989) and (b) sample location map.

CATHLES, 1979). However, the results from recent geochronologic studies at the Panasqueira Sn-W deposit, Portugal (SNEE et al., 1988) and the Cornubian metalliferous-province, England (HALLIDAY, 1980; DARBYSHIRE and SHEPHERD, 1985; CHESLEY et al., 1991) suggest that this hypothesis may be an oversimplification and that granite-related mineralization may postdate the host granite pluton by 5 to 35 myrs. Although models have been proposed for long-lived fluid circulation driven by elevated radioelement heat production in southwest England (SIMPSON et al., 1979; DURRANCE et al.,

1982), these models can only explain lower temperature fluid circulation and cannot account for the 200 to 400°C fluids observed at either southwest England or at Panasqueira (SHEPHERD et al., 1985). If hydrothermal circulation is indeed long-lived or significantly postdates known plutonic activity, then we should re-examine some of the fundamental interpretations regarding pluton formation and granite-related mineralization. For example, what are the time spans and mechanisms for the generation and emplacement of composite intrusives and silicic magmas? How important is the duration of batholith and pluton emplacement in the generation of an ore deposit? What is the driving force for hydrothermal circulation? Is hydrothermal circulation episodic or continuous?

The classic Cornubian Sn-bearing granites of southwest England (Fig. 1a) have provided a natural laboratory for the development of many early theories of granite emplacement and related mineral deposition (e.g., PRYCE, 1778; DE LA BECHE, 1839; DAVISON, 1927; DINES, 1956). Well-documented geologic and paragenetic relations make the Cornubian batholith an ideal setting for a detailed geochronologic study of the relation between mineralization and plutonism.

In this study, U-Pb isotopic ages of monazite and xenotime are compared with $^{40}Ar/^{39}Ar$ ages of hornblende and primary muscovite (muscovite was determined to be primary using the criteria of MILLER et al., 1981) from skarns and individual plutons within the Cornubian batholith in order to assess both the magmatic history of the batholith and the cooling rate of individual plutons. In addition, $^{40}Ar/^{39}Ar$ muscovite ages from mineralized veins and Sm-Nd isochron ages of fluorite from the main stage of mineralization are used to quantify the lifetime of the Cornubian mineralizing system(s). None of the current models for granite emplacement and mineralization adequately explain the emplacement, cooling, and mineralization histories established by these isotopic age determinations.

BACKGROUND GEOLOGY

The Cornubian batholith was emplaced at the end of the Hercynian Orogeny (Carboniferous to Permian), which involved the continental collision of what is now northern and southern Europe (e.g., STONE and EXLEY, 1985). The batholith has a strike length of 250 km and a maximum width of 50 km, extending from Dartmoor in the northeast to the Isles of Scilly in the southwest (Fig. 1a). There are five major plutons and a number of satellite granite bodies which comprise the majority of the exposed batholith. The batholith consists predominantly of coarse-grained, peraluminous, biotite, and biotite-muscovite granites similar to the S-type granites of CHAPPELL and WHITE (1974). They intrude folded, weakly metamorphosed Devonian and Carboniferous sedimentary and mafic igneous rocks, resulting in a thermal overprint and metasomatism of the country rocks which produced a range of lithologies including hornfels, tourmalinized slates, and garnet-pyroxene-amphibole skarns.

Several workers have classified the granites in the Cornubian batholith on the basis of mineralogy, texture, and chemistry (e.g., HAWKES and DANGERFIELD, 1978; EXLEY and STONE, 1982; EXLEY et al., 1983; STONE and EXLEY, 1985; HILL and MANNING, 1987). Xenoliths of granitic to granodioritic composition are found within some of the main plutons and are considered to represent the disrupted remains of earlier episodes of plutonism. Approximately 90% of the exposed granite is a coarse-grained biotite-muscovite granite (CGBG), with turbid megacrysts of potassium-feldspar in a finer grained, equigranular matrix of quartz, plagioclase, biotite, muscovite, and tourmaline. Although volumetrically minor, four later episodes of granite magmatism have been recognized (EXLEY et al., 1983): fine-grained biotite granite; megacrystic Li-mica granite; fine-grained Li-mica granite (topaz granite of MANNING and HILL, 1990), and fluorite granite. The different granite lithologies are not observed within each pluton, but all of the plutons are composite in nature.

Crosscutting some of the major granite plutons are a series of vertical to near vertical felsic porphyry dikes, locally called elvans. DANGERFIELD and HAWKES (1969) suggested that the dikes represent contemporaneous felsic volcanism. Other workers have considered the elvans to be the last stage of magmatism in the Cornubian batholith and separate the elvans (280–270 Ma) from the plutons (290–280 Ma) in time (DARBYSHIRE and SHEPHERD, 1985), or suggest that the elvans represent crystallized and degassed products extracted from the main CGBG residuum derived from deep within the batholith (JACKSON et al., 1989; WILLIS-RICHARDS and JACKSON, 1989). Minor and trace element chemistry suggest that the elvans are genetically linked to the CGBG granites (DARBYSHIRE and SHEPHERD, 1985). Many authors proposed a temporal link between the mineralization and the emplacement of the elvans (e.g., HALLIDAY, 1980; JACKSON et al., 1982, 1989; DARBYSHIRE and SHEPHERD, 1985), because the elvans utilize the same fracture systems as the mineralizing fluids and indicate the presence of a magmatic heat source young enough to produce high-temperature tin mineralization.

Mineralization is associated with multiple, steeply-dipping fractures and lodes that crosscut both the granites and country rocks. The lodes are as much as several km in length and average 0.5–2 m in width (JACKSON et al., 1989). Ore-bearing lodes typically exhibit evidence of multiple episodes of mineralizing fluids, accompanied by subtle changes in fluid chemistry. Early workers attributed mineral zoning to simple cooling of a fluid from a single emanative center (e.g., DINES, 1956), but later workers recognized the overlapping polyascendent nature of the mineralization and the telescoped zoning of the ores (e.g., GARNETT, 1965; JACKSON et al., 1982). Presently, most researchers recognize four major stages of granite-related mineralization (e.g., STONE and EXLEY, 1985; SHEPHERD et al., 1985; Table 1):

1) The earliest recognized mineralization features are exoskarns produced by metasomatism of pelitic shales and metabasalts during granite intrusion (JACKSON et al., 1982; VAN MARCKE DE LUMMEN and VERKAEREN, 1985; SCRIVENER et al. 1987). Exo-

Table 1. Mineralization Paragenesis in Cornwall, England.

	Stage 1	Stage 2		Stage 3	Stage 4
Style	Skarns.	Pegmatitic Deposits.	Sheeted Greisen Bordered Veins. Tourmaline Bearing Veins.	Sn-Bearing Polymetallic Fissure Veins. Predominantly East-West.	Late Polymetallic Sulfide Veins. "Crosscourse" Predominantly North-South.
Economic Metals	Fe, Cu, Sn	Sn, W ± Mo	Sn, W	Sn, Cu, Pb, Zn, As, Fe	Pb, Zn, Ag, Fe, Sb U.
Gangue Minerals	Gnt., Px., Tourm., Amph.,	Qz., Fsp., Musc., Tourm.	Qz., Musc., Tourm.	Qz., Fsp., Chl., Hem., Fluor.	Qz., Bar., Dol., Calc., Fluor.
T_h (°C)	375° - 450°	300° - 500°	300° - 500°	200° - 400°	100° -170°

skarn minerals include garnet, pyroxene, epidote, Cl-rich amphiboles, malayaite, vesuvianite, siderite, and axinite. The skarns contain economic concentrations of Sn, Cu, Fe, and As; fluid inclusion homogenization temperatures (T_h) have been reported to range from 260–475°C. (JACKSON et al., 1982; SCRIVENER et al., 1987).

2) An early episode of mineralized pegmatites, greisen-bordered veins and Sn-tourmaline veins and breccias containing predominantly tin and tungsten oxides; T_h ranges from 300°–500°C. Tourmaline is coeval with the cassiterite and is the main gangue mineral. SHEPHERD et al. (1985) recognized a bimodal population of fluid inclusions, which was interpreted as unmixing of early high-temperature magmatic fluids into a low-salinity, high CO_2, W ± Sn-bearing fluid and a high-salinity, low CO_2 Sn-bearing fluid.
3) The main episode of mineralization consists of polymetallic quartz-tourmaline-chlorite-sulfide-fluorite-bearing fissure veins which trend predominantly east-west. The veins contain Sn, Cu, Pb, Zn, Fe, and As-sulfides ± SnO_2 and give T_h values of 200–380°C (JACKSON, 1977; JACKSON et al., 1982; SHEPHERD et al., 1985; SHEPHERD and SCRIVENER, 1987). Stage 3 veins represent the major period of economic mineralization in Cornwall. Gangue minerals are dominantly chlorite with minor tourmaline. The mineralogical zoning, high fluid inclusion homogenization temperatures and structures of these ore bodies, together with their apparent spatial relations with the granite led to the traditional view that this stage of mineralization was related to emanative centers within the host pluton (DINES, 1956).
4) The last stage of mineralization consists of polymetallic (Pb, Zn, Ag, and U) quartz-fluorite-barite-sulfide veins, locally termed crosscourses. Fluid inclusions yield T_h values of 105–180°C (JACKSON, 1977; JACKSON et al., 1982; SHEPHERD et al., 1985; SHEPHERD and SCRIVENER, 1987). These fluids are similar in composition to Na-Ca-Cl-rich deep sedimentary brines and have been suggested to be the result of fluid expulsion from adjacent Mesozoic sedimentary basins (ALDERTON, 1975, 1978; SHEPHERD et al., 1985).

An economically important feature of the southwest England granites is the widespread but localized presence of intense hydrothermal kaolinization (china clay). Kaolinization is centered on the western portion of the St. Austell granite, southern Dartmoor granite and smaller workings on other plutons. The age and genesis of the kaolin deposits is still a matter of debate (e.g., SHEPPARD, 1977; DURRANCE et al., 1982; EXLEY et al., 1983), but they are commonly thought to be the result of meteoric fluid circulation during the late stages of cooling of the Cornubian batholith.

Stage 1, 2, and 3 mineralization have been directly attributed to the intrusion and cooling of the Cornubian batholith. Although the stage 4 low-temperature fluids may not be linked directly to intrusion and cooling of the batholith, a model involving low-temperature, regional fluid-convection driven by the high-heat production of the granite batholith has been proposed (DURRANCE et al., 1982).

Previous geochronologic studies of the Cornubian batholith and associated mineral deposits are numerous and exhibit a high variability in the measured ages (see WILLIS-RICHARDS and JACKSON, 1989, for summary of ages). A detailed Rb-Sr study of the major and minor plutons by DARBYSHIRE and SHEPHERD (1985, 1987) established a two-stage emplacement for the batholith, with an age of 290–280 Ma for major granite magmatism and an age of 280–270 Ma for the minor rhyolite porphyry dikes and chemically specialized granites. Mineralization ages from the Sn-bearing lodes also exhibit a high degree of scatter ranging from 294–259 Ma (see WILLIS-RICHARDS and JACKSON, 1989, for summary of ages). Rubidium-strontium fluid inclusion ages of 269 ± 4 Ma (DARBYSHIRE and SHEPHERD, 1985) and Sm-Nd fluorite ages 259 ± 7 Ma (CHESLEY et al., 1991) have been reported for the Stage 3 mineralization in the South Crofty mine and postdate the host Carnmenellis pluton by 30–40 myrs, suggesting that mineralization must be linked to later igneous activity. $^{40}Ar/^{39}Ar$ and K-Ar ages for clay concentrates suggest that lower temperature hydrothermal solutions were active during the Mesozoic and Cenozoic (JACKSON et al., 1982).

SCIENTIFIC METHODOLOGY

To determine the emplacement and cooling history of the Cornubian batholith and its effect on hydrothermal circulation, it is necessary to obtain an accurate measurement of (1) the lifetime of magmatism within the batholith as well as individual plutons and (2) the time taken for the plutons to cool below temperatures where they were no longer capable of driving 200–400°C mineralizing fluids.

The closure temperature for different isotopic systems in different minerals provides a quantitative evaluation of the cooling history of an igneous or metamorphic terrane. In order to resolve the cooling rate of a pluton, the pluton must have cooled slowly enough so that the elapsed time between ages for different minerals with different closure temperatures is greater than the analytical uncertainty in the age. A detailed explanation of closure temperature theory and models is available in DODSON (1973), GANGULY and RUIZ (1987) and MCDOUGALL and HARRISON (1988).

Normally, U-Pb ages from zircons are used to provide the best age of emplacement for a magmatic body. However, the Cornubian granites were formed by melting of a source with a significant sedimentary component (e.g., HAMPTON and TAYLOR, 1983), therefore, the zircons will likely contain inherited radiogenic Pb (see also Fig. 2). Monazite appears to lose Pb by volume diffusion during high-temperature metamorphic or melting events (PARRISH, 1990). Hence, inherited Pb is seldom observed in granites. Although there have been no rigorous experimental determinations of the closure temperature for Pb, PARRISH (1990) has estimated the closure temperature to be 725° ± 25°C from a variety of studies in metamorphic and igneous terranes. Estimates for the closure temperature for Pb in xenotime are scarce, but it is considered to be ~650°C by HEAMAN and PARRISH (1991). The presence of primary andalusite and muscovite suggest that crystallization temperatures were <750°C (e.g., KERRICK, 1990). Therefore, a more accurate and reliable emplacement age can be obtained from U-Pb dating of monazite and xenotime. The U-Pb data for Th-rich minerals such as monazite commonly are reversely discordant (e.g., PARRISH, 1990). This discordance is generally thought to be the result of incorporation of excess/unsupported ^{206}Pb that formed from ^{230}Th incorporated during the formation of the mineral (SCHÄRER, 1984). In most cases, it has been demonstrated that the $^{207}Pb/^{235}U$ ages can be accepted as geologically correct (SCHÄRER, 1984; PARRISH, 1990). Therefore, only the $^{207}Pb/^{235}U$ age of the monazite is used for a thermochronologic comparison of ages in this study. Monazite has been shown to retain Pb during low-temperature melting events (COPELAND et al., 1988). To evaluate whether any differences between the U-Pb monazite and $^{40}Ar/^{39}Ar$ muscovite ages could be the result of inherited Pb, replicate U-Pb analyses were made of different size euhedral grains from the same monazite sample (Table 2). The ages are in good agreement for the different size fractions and do not indicate inheritance of Pb in any sample.

Muscovite K-Ar closure temperatures have been estimated from the literature to be 320° ± 40°C (SNEE, 1982). SNEE et al. (1988) independently estimated a similar temperature for closure of muscovite to Ar diffusion of ~325°C, based on fluid inclusion filling temperatures at the Panasqueira mine. Using regressions of both laboratory and geologic data, HARRISON (1981) and MCDOUGALL and HARRISON (1988) calculated a K-Ar closure temperature of 525° ± 25°C for hornblende in a pluton cooling at a rate of 100°C myr^{-1} and demonstrated that the closure temperature for rapidly cooled hornblendes (1000°C myr^{-1}) would be higher (~580°C). One of the strengths of $^{40}Ar/^{39}Ar$ dating lies in the ability to resolve an age using step-wise degassing to determine a plateau or the average of a portion of an age spectrum whose ages overlap at the 2σ level. The majority of the samples presented here exhibit an age plateau using the widely accepted and published definition for the term (e.g., DALRYMPLE and LANPHERE, 1974; FLECK et al., 1977). In order to compare the $^{40}Ar/^{39}Ar$ plateau-ages with those of other muscovites and U-Pb ages of monazite or xenotime, the plateau criteria have been expanded to conform to those of SNEE et al. (1988) and the errors are reported at the 95% confidence level. Samples that failed the criteria for a plateau were also reduced using the isochron (YORK, 1969) and correlation diagram methods (RODDICK et al., 1980).

Several biotite fractions were analyzed for $^{40}Ar/^{39}Ar$. Most of the data define hump-shaped age-spectra that do not fit the criteria for a plateau. The total gas age is similar to the plateau-ages for corresponding muscovites, but in most cases it is slightly older. Many of the biotites exhibit weak chloritization in thin section; despite efforts to obtain clean biotite separates, chlorite may be present in the sub-

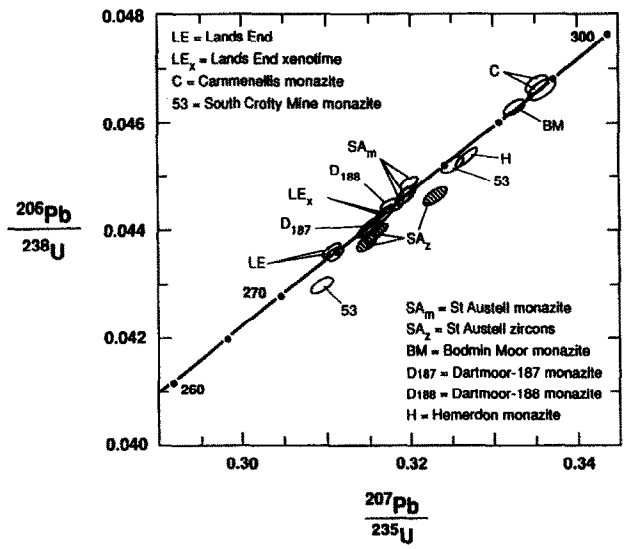

FIG. 2. Concordia diagram for monazite, xenotime and zircon separates from plutons in the Cornubian batholith. Error ellipses are drawn using 2σ error.

microscopic level. The $^{40}Ar/^{39}Ar$ analyses of biotite samples are reported, but are not used for interpretation of the thermal history of the Cornubian plutons.

Sample locations are plotted on an outline map of the Cornubian granites (Fig. 1b). A list of sample locations and lithologic descriptions can be found in Appendix 1.

ANALYTICAL TECHNIQUES

Monazite, zircon, and xenotime were separated from crushed granite specimens using standard separation techniques. Between twenty and fifty grains were hand-picked under a binocular microscope on the basis of size, color, lack of inclusions and shape and subsequently washed in boiling deionized water for 2–3 h to remove surface contamination. Representative sub-samples of the hand-picked separate were examined on the microprobe with Energy Dispersive System (EDS) and Back-Scattered Electron (BSE) imaging to assure identity and purity. After spiking with a mixed ^{235}U-^{205}Pb tracer the samples were dissolved in distilled 6 N HCl or concentrated HF and 7 N HNO_3, in a 3 ml Teflon® vial inside a Krogh-style Teflon® vessel at 210°C for 3–5 days. The Pb was purified using standard HBr-HCl chemistry on BioRad AG1-X8 200–400 mesh resin. The U was purified using HCl-HNO_3-H_2O chemistry on the same columns (TILTON, 1973; MATTINSON, 1986; MANHES et al., 1984; PARRISH et al., 1987). Samples were corrected for common Pb using the feldspar analyses of HAMPTON and TAYLOR (1983) for the different plutons in the Cornubian batholith. Due to the high $^{206}Pb/^{204}Pb$ ratios of most samples the effect of the common Pb correction is negligible. The measured ratios were corrected for a total procedural Pb blank of 40–200 pg. Isotopic compositions of Pb and U were determined in the static mode on a VG Sector mass spectrometer equipped with an ion-counting Daly detector. The reproducibility of the $^{207}Pb/^{206}Pb$ ratio for the standard was 0.06% (2σ). The U total process blanks were less than 10 pg during the period of analysis. The 2σ uncertainty of the U-Pb and $^{207}Pb/^{206}Pb$ ages include the reproducibility of the standard, common Pb, and blank corrections as well as within-run uncertainties and the uncertainties in the U/Pb ratio of the spike.

Minerals for $^{40}Ar/^{39}Ar$ analysis were separated from the same crushed samples used for U-Pb determinations using standard methods. Subsequently, the separates were hand-picked under a binocular microscope to better than 99% purity. Between 10 and 40 mg of each sample was enclosed in an Al-foil capsule and placed along with MMhb-1 hornblende standard (SAMSON and ALEXANDER, 1987), CaF_2 and K_2SO_4 in evacuated quartz vials. The samples were irradiated in two separate packages at 1 MW for 30 and 40 hours, respectively, while being continually rotated in the central thimble of the TRIGA research reactor at the USGS in Denver, Colorado (DALRYMPLE et al., 1981). The MMhb-1 monitor was distributed evenly within the quartz vials in order to obtain a precise monitoring of both the horizontal and radial flux gradients; every sample was adjacent vertically to at least one standard. Data from MMhb-1 monitors show an error in the J-value of 0.1% (1σ) for both packages. The samples were analyzed in the static mode on a MAP 215 mass spectrometer with a Nier-type source at the USGS in Denver (GEISSMAN

Table 2. U-Pb Analytical Results

Sample #	Lithology (Mineral*)	Diameter (μm)#	U ppm	Pb ppm	Atomic Ratios $^{206}Pb/^{204}Pb$	$^{208}Pb/^{206}Pb$	$^{207}Pb/^{206}Pb$	2σ (%)	$^{206}Pb/^{238}U$	2σ (%)	$^{207}Pb/^{235}U$	2σ (%)	Ages(Ma) $^{206}Pb/^{238}U$	2σ	$^{207}Pb/^{235}U$	2σ	$^{207}Pb/^{206}Pb$
Lands End																	
JTC-135S-89	FGBG (Xe)	50-100, e	5155	274	3916	0.3408	0.05185	(0.08)	0.0442	(0.25)	0.3166	(0.26)	279.3	[0.7]	279.3	[0.6]	279.2
JTC-135L-89†	(Xe)	150-200, e	22105	959	19535	0.0087	0.05184	(0.07)	0.0442	(0.25)	0.3164	(0.26)	279.3	[0.7]	279.2	[0.6]	278.6
JTC-136S-89	CGBG (Mz)	20-50, e	2579	413	1664	3.172	0.05177	(0.10)	0.0435	(0.25)	0.3109	(0.27)	274.9	[0.7]	274.9	[0.6]	275.3
JTC-136L-89	(Mz)	60-100, e	6778	875	2495	2.350	0.05162	(0.10)	0.0436	(0.27)	0.3105	(0.29)	275.3	[0.7]	274.6	[0.7]	268.8
Carnmenellis																	
JTC-53-89	CGBG (Mz)	20-40, e	329	46.0	761.2	2.680	0.05223	(0.20)	0.0429	(0.26)	0.3095	(0.35)	271.3	[0.7]	273.8	[0.8]	295.5
JTC-53-89	Mz	50-100, e	1075	234	1236	4.477	0.05217	(0.12)	0.0452	(0.24)	0.3254	(0.28)	285.2	[0.7]	286.1	[0.7]	293.0
JTC-242-89	CGBG (Mz)	20-70, e	4856	874	1575	3.345	0.05202	(0.15)	0.0467	(0.25)	0.3351	(0.29)	294.4	[0.7]	293.5	[0.7]	286.4
JTC-81-89	CGBG (Mz)	20-50, e	6069	1474	2672	4.925	0.05223	(0.24)	0.0466	(0.29)	0.3357	(0.37)	293.8	[0.8]	294.0	[1.0]	295.7
St Austell																	
JTC-276S-89	CGBG (Mz)	20-50, e	782	130	3443	3.228	0.05171	(0.10)	0.0448	(0.26)	0.3200	(0.28)	283.1	[0.7]	282.0	[0.7]	272.9
JTC-276M-89	(Mz)	50-150, e	1782	303	1622	3.306	0.05192	(0.10)	0.0446	(0.25)	0.3196	(0.27)	281.6	[0.7]	281.6	[0.7]	282.0
JTC-276L-89	(Mz)	>200, b	6984	451	2719	0.6087	0.05189	(0.08)	0.0446	(0.26)	0.3197	(0.27)	281.8	[0.7]	281.7	[0.7]	280.9
JTC-276C-89	(Zr)	c, e, u, 10:1	352	15.5	670.0	0.007836	0.05249	(0.19)	0.0446	(0.28)	0.3230	(0.35)	281.5	[0.8]	284.3	[0.9]	307.9
JTC-276T-89	(Zr)	c, e, u, 5:1	255	10.7	986.3	0.005532	0.05215	(0.17)	0.0437	(0.25)	0.3146	(0.32)	276.1	[0.7]	277.8	[0.8]	292.0
JTC-276B-89	(Zr)	c, e, b	731	31.1	1423	0.006869	0.05215	(0.12)	0.0439	(0.34)	0.3158	(0.37)	277.1	[0.9]	278.7	[0.9]	292.2
Bodmin Moor																	
JTC-312-89	CGBG (Mz)	20-50, e	3074	571	678.0	3.444	0.05205	(0.14)	0.0463	(0.27)	0.3324	(0.30)	291.9	[0.8]	291.4	[0.8]	287.9
Dartmoor																	
JTC-187-89	CGBG (Mz)	50-100, e	2574	366	2211	2.664	0.05184	(0.10)	0.0440	(0.32)	0.3151	(0.34)	278.1	[0.9]	278.2	[0.8]	278.5
JTC-188-89	CGBG (Mz)	20-75, e	780	128	146.6	2.639	0.05185	(0.31)	0.0445	(0.25)	0.3183	(0.47)	280.8	[0.7]	280.6	[1.2]	279.0
Hemerdon																	
JTC-318B-89	CGBG (Mz)	20-50, e	1065	174	1215	3.067	0.05229	(0.11)	0.0453	(0.30)	0.3270	(0.32)	285.9	[0.8]	287.3	[0.8]	298.3

CGBG = Coarse-grained biotite granite; FGBG = Fine-grained biotite granite

* Mz= Monazite, Xe=Xenotime, Zr=Zircon.

c=clear, b=broken, u=unbroken, e=euhedral, length:width.

$^{206}Pb/^{204}Pb$ measured ratios, All other isotopic ratios corrected for blank spike, common lead and fractionation.

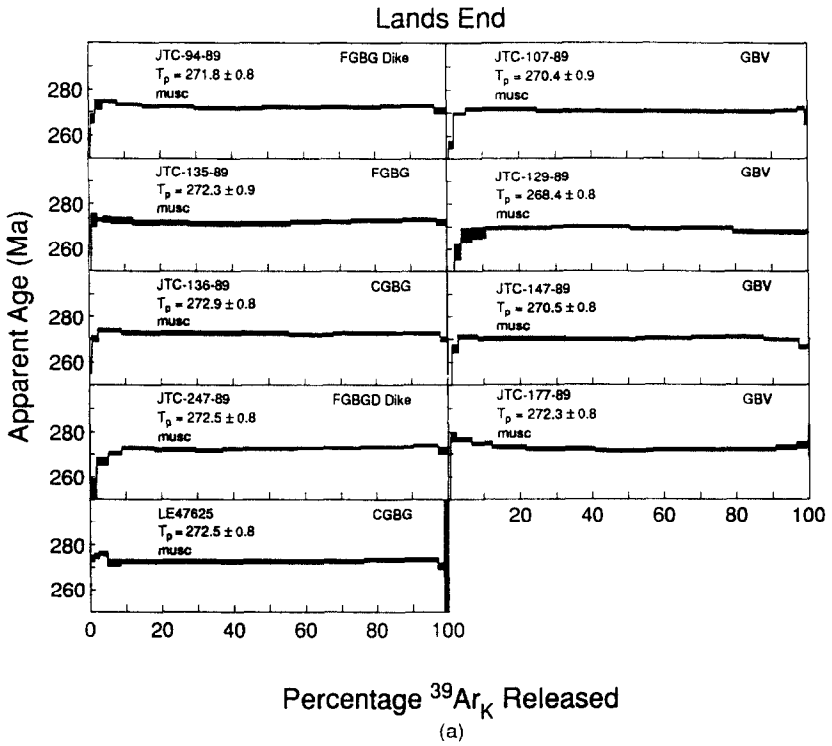

(a)

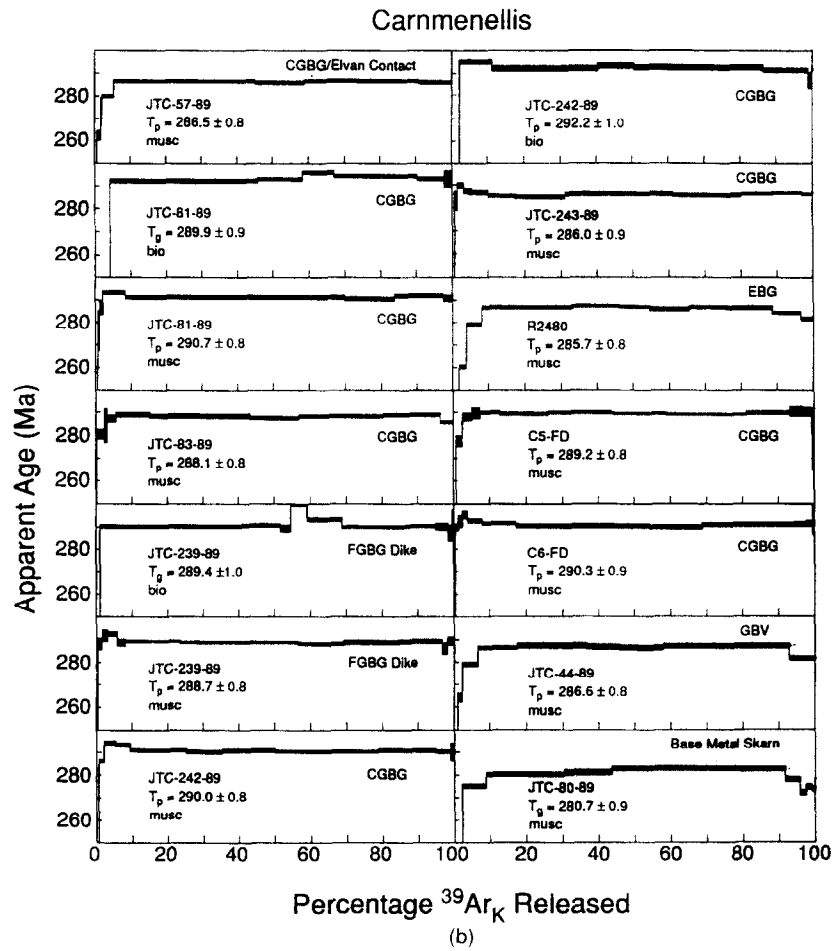

(b)

FIG. 3a-g. $^{40}Ar/^{39}Ar$ release spectra for primary and secondary muscovite (musc), biotite (bio) and hornblende (hbld) from plutons, skarns and mineralized veins in southwest England. CGBG = Coarse-grained biotite-granite; FGBG = fine-grained biotite granite; EBG = equigranular biotite granite; GBV = greisen bordered vein; T_g = total gas age; T_p = Total plateau age; all spectra are plotted using the 2σ error in the age; see text and Table 3 for explanation. Data for the Ar analyses will be available as a U.S. Geological Survey Bulletin (in prep.).

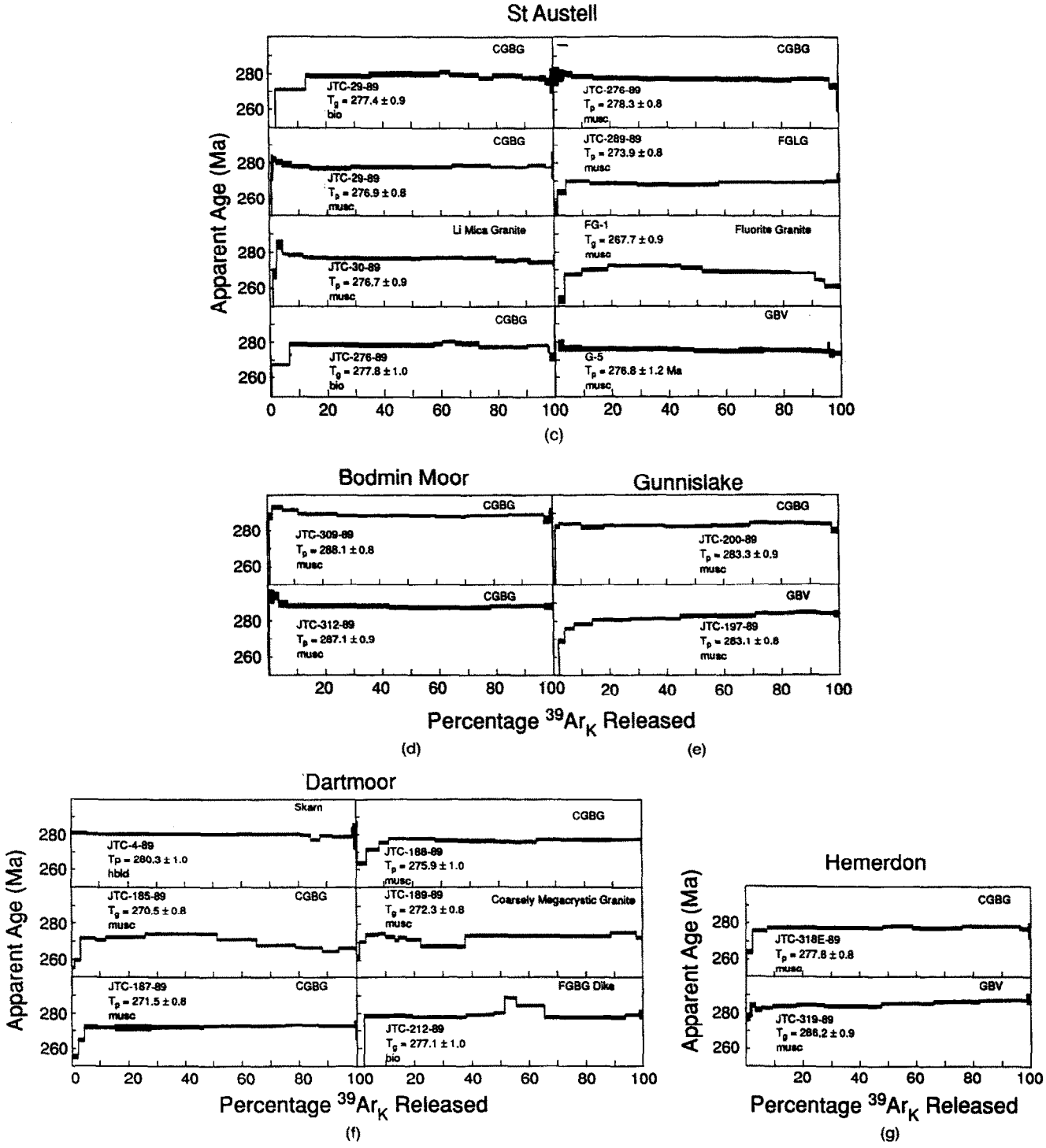

FIG. 3. (Continued)

et al., 1992). Analyses were made on a single faraday collector; detection limit during the period of analyses was 2×10^{-17} moles Ar. Corrections were applied for interferences from the reaction products of Ca, Cl, and K and from the decay of ^{37}Ar. Uncertainties for all ages are quoted at the 2σ confidence level and include the estimated error in J.

The techniques for the Sm-Nd fluorite analyses are given in CHESLEY et al. (1991). All data were reduced using the decay constants and isotopic abundances recommended by STEIGER and JÄGER (1977) and an age of 520.4 Ma for MMhb-1 (SAMSON and ALEXANDER, 1987). Isochrons, concordia plots, and weighted average calculations were performed using ISOPLOT (LUDWIG, 1991).

ANALYTICAL RESULTS

The results of U-Pb, $^{40}Ar/^{39}Ar$, and Sm-Nd analyses are presented in Tables 2, 3, and 4. The U-Pb data are plotted on a standard concordia diagram (Fig. 2); a U-Pb analysis is considered concordant only if there is substantial overlap with concordia at the 2σ level. Argon age-spectra are plotted in Fig. 3 and the Sm-Nd isochrons are plotted in Fig. 4. A summary of the U-Pb, $^{40}Ar/^{39}Ar$, and Sm-Nd data from this study for the Cornubian batholith is presented in Fig. 5.

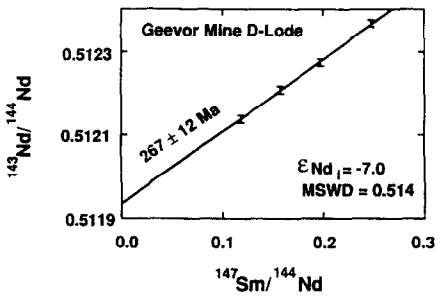

FIG. 4. Sm-Nd isochron diagram for the Geevor Mine D-lode. The fluorites are plotted as 2σ mean error bars; see text for discussion.

Lands End Pluton

Two samples were analyzed for U-Pb from the Lands End pluton: a fine-grained biotite-granite (sample 135) and a coarse-grained biotite-granite (CGBG), typical of the Lands End pluton (sample 136). The fine-grained biotite granite, 4 × 6 km in outcrop, is considered to be either a younger intrusion equivalent to the fine-grained granites observed to crosscut the CGBG at depth in the Geevor Mine (MOUNT, 1985), or alternatively a roof pendant of earlier granite within the main CGBG of the Lands End pluton. The weighted average $^{207}Pb/^{235}U$ age is 279.3 ± 0.4 Ma for xenotime from the fine-grained granite (135) and 274.8 ± 0.5 Ma for monazite from the main CGBG (136). Although the U-Pb ages differ by approximately 4 myrs, the corresponding muscovites give indistinguishable $^{40}Ar/^{39}Ar$ plateau-ages of 272.3 ± 0.9 Ma and 272.9 ± 0.8 Ma, respectively. The difference in U-Pb ages, the estimated lower closure temperature (~650°C) for xenotime compared to monazite (HEAMAN and PARRISH, 1991), and the similarity in $^{40}Ar/^{39}Ar$ ages suggest that the muscovite from the fine-grained granite has been reset or was above the Ar closure temperature at the time the main CGBG was intruded. Combined with reports from a drill hole which passed vertically through the fine-grained granite into the main CGBG (REID and FLETT, 1907), these results indicate that the fine-grained granite is probably a roof pendant of an earlier igneous phase. A total of five muscovite samples from the Lands End pluton were analyzed by the $^{40}Ar/^{39}Ar$ method: two from the main CGBG (136, LE47625), and the fine-grained granite dikes (94, 247); one from fine-grained granite (135). All of the samples overlap within error and yield a weighted average age of 272.4 ± 0.4 Ma. The similarity in cooling ages throughout the pluton, in the aureole and at depth may indicate regional cooling of the Lands End area possibly produced through cooling promoted by hydrothermal convection. A cooling rate of ~210°C myr^{-1} can therefore be calculated from the age difference (1.9 myr) between closure of monazite to Pb at ~725°C and muscovite closure to Ar at ~325°C. If the fine-grained granite dikes are cogenetic with the crosscutting granite observed in the Geevor mine, then a minimum emplacement age for the fine-grained granite is implied.

A comparison of our results with the Rb-Sr data provided by DARBYSHIRE and SHEPHERD, (1985, 1987) for the batholith provides a test of their original interpretation and con-

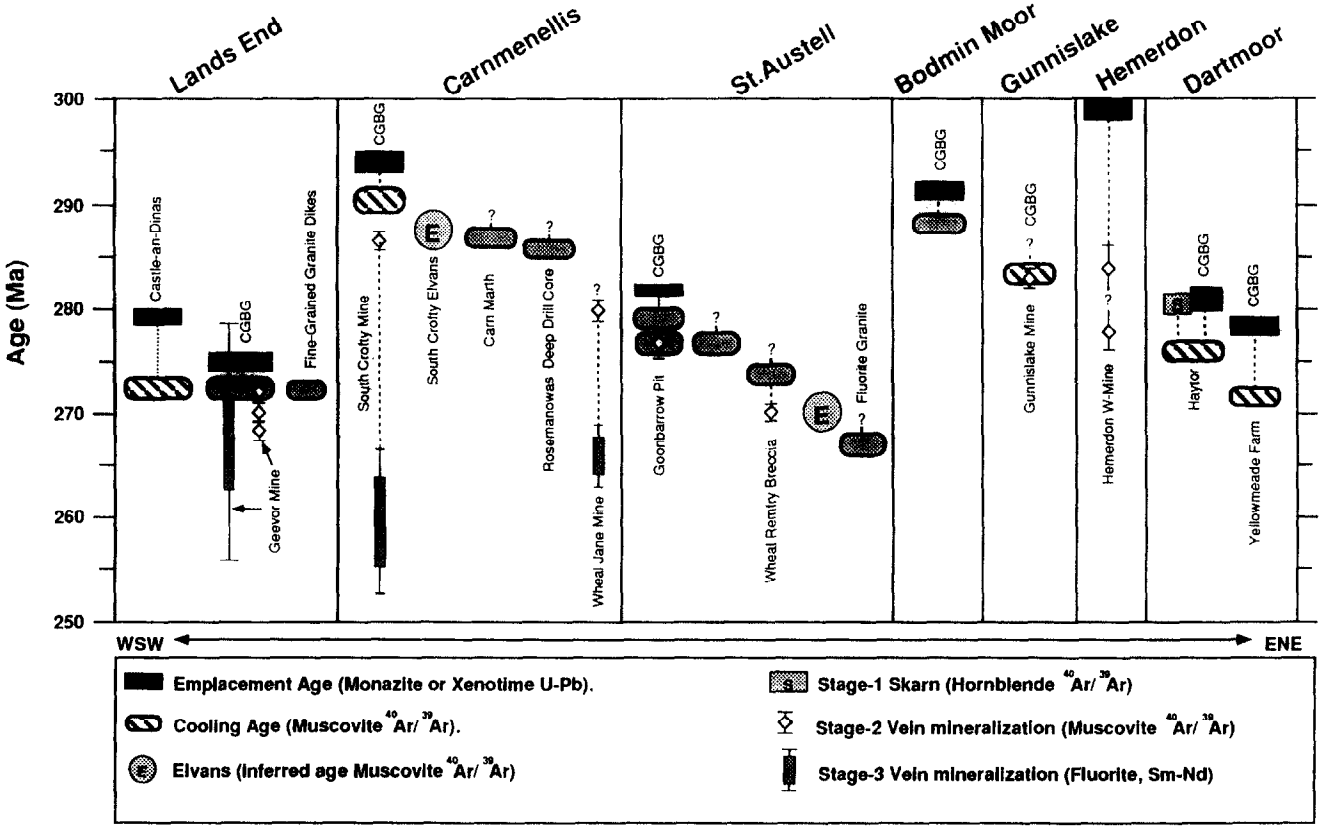

FIG. 5. Compilation of all geochronologic data (this study) for the Cornubian batholith. The symbols include the 2σ error in the age.

tributes to the understanding of the relationship between Rb-Sr, U-Pb, and $^{40}Ar/^{39}Ar$ isotopic systems. They obtained a whole-rock Rb-Sr isochron age of 268 ± 2 Ma for the Lands End granite. Based on a Rb-Sr whole-rock isochron age for the Wherry elvan of 282 ± 6 Ma, which is thought to crosscut the metamorphic aureole of the Lands End granite and a Rb-Sr mineral-age of 279 ± 4 Ma from a crosscutting greisen bordered quartz vein in the granite (HALLIDAY, 1980), DARBYSHIRE and SHEPHERD (1985) concluded that the Rb-Sr systematics of the Lands End granite had been reset from an older age (290–280 Ma). However, the younger monazite and xenotime U-Pb ages and agreement with the $^{40}Ar/^{39}Ar$ muscovite ages with respect to closure temperature, suggest that the Lands End granite was not reset from an older age.

Four samples from mineralized veins or lodes which contain secondary muscovite were analyzed from the Geevor Mine and the Bostraze china clay pit. The secondary muscovite is generally anhedral and occurs as a replacement of K-feldspar, as replacement rims on biotite and within quartz-tourmaline veinlets. A secondary muscovite from a high temperature (400–460°C; JACKSON et al., 1982), sheeted greisen-bordered vein in the Bostraze clay pit (177) gives a plateau-age of 272.3 ± 0.9 Ma (Table 3), which is indistinguishable from the muscovite cooling ages for the host main CGBG (272.7 ± 0.8 Ma). Although the sample passes the criteria for a plateau, the total spectrum exhibits some features that may indicate disturbance (Fig. 3a), possibly by the lower temperature clay forming event. The age most likely represents a minimum age for the stage 2 mineralization contemporaneous with the cooling of the host granite below muscovite closure to Ar. Secondary muscovite from altered host CGBG on the contact of the Simms lode (107), the CGBG on the hanging wall contact of the Coronation lode (147) and the crosscutting, fine-grained granite along the Coronation lode (129) in the Geevor mine yield slightly younger plateau-ages of 270.4 ± 0.9 Ma, 270.5 ± 0.8 Ma, and 268.4 ± 0.8 Ma, respectively, and are distinct in age from primary muscovites from the host pluton. The overlapping nature of the mineralization (GARNETT, 1965; JACKSON et al., 1982) and the distinct ages imply that stage 2 and stage 3 mineralization was long-lived and occurred over a minimum period of 2–4 myrs. The age for stage 3 polymetallic mineralization is corroborated by a fluorite Sm-Nd isochron age of 267 ± 12 Ma (2σ) (Fig. 4). The above results are also consistent with a previously determined Rb-Sr isochron mineralization age of 270 ± 2 Ma (JACKSON et al., 1982).

Carnmenellis Pluton

The Carnmenellis pluton is composed of several distinct phases of granite intrusion (GHOSH, 1934) and has two small satellite intrusions, the Carn Marth, and Carn Brea granites (Fig. 1a). The Carn Brea granite is observed to be in contact with the Carnmenellis pluton at depth (TAYLOR, 1969) and the Carn Marth granite is considered a separate intrusion (HILL and MACALISTER, 1906). Two monazite samples from quarries (81, 242) in the Carnmenellis granite and one from the South Crofty Mine in the Carn Brea granite (53) were dated by the U-Pb method (Table 2; Fig. 2). The age of sample 81 is concordant, but the analysis of sample 242 is reversely discordant beyond analytical uncertainty, most likely due to the incorporation of excess ^{230}Th. The weighted average of the $^{207}Pb/^{235}U$ ages is 293.7 ± 0.6 Ma and is taken as the best estimate for the emplacement age. Data for two separates of monazite from sample 53 are discordant. However, the $^{207}Pb/^{206}Pb$ ages of ~293 and ~295 Ma are in excellent agreement with the emplacement age determined for the Carnmenellis granite. These monazites most likely represent partial disturbance associated with the stage 2 and 3 high-temperature hydrothermal fluids at the South Crofty Mine.

The muscovites from samples 81 and 242 give ages of 290.7 ± 0.9 and 290.0 ± 0.8 Ma, respectively, and correspondingly yield a cooling interval of 3.1 and 3.3 myrs (~125°C myr^{-1}) from emplacement to muscovite closure for Ar. Sample 239 is from a fine-grained granite dike and yields an age of 288.7 ± 0.8 Ma. Samples 57 and 83 were collected in the Carn Brea granite in close proximity to elvan dikes in the South Crofty mine and give younger $^{40}Ar/^{39}Ar$ plateau-ages of 286.5 ± 0.9 Ma and 285.4 ± 0.9 Ma, respectively. Both ages overlap and are younger than the cooling age of ~290 Ma for the Carnmenellis pluton suggesting that they were reset by the emplacement of the elvan. Sample 243 from the Carn Marth granite gives a plateau age of 286.0 ± 0.9 Ma. This age suggests a separate cooling history postdating that of the Carnmenellis pluton by about 4 myrs. The idea of a separate intrusion is supported by the field relations (HILL and MACALISTER, 1906) and the more evolved geochemistry (CHAROY, 1986) of the Carn Marth granite. Sample R2480 is from an equigranular granite of unknown dimension intersected in the Hot Dry Rock deep borehole (Rosmanowas quarry) in the Carnmenellis granite. The muscovite gives a plateau age of 285.7 ± 0.9 Ma suggesting significantly slower cooling or a separate pulse of granite magma.

In contrast to the Lands End granite, it is clear that the Carnmenellis pluton underwent a more protracted cooling history which was affected by multiple intrusive events postdating initial emplacement and cooling. The geochronology supports field observations by GHOSH (1934) who suggested several discrete episodes of granitic magmatism in the Carnmenellis area. As in Lands End, there is an excellent agreement between the $^{40}Ar/^{39}Ar$ plateau-ages (289.2 ± 0.8 and 290.3 ± 0.9 Ma) and the Rb-Sr mineral isochron ages (287 ± 2 Ma. and 290 ± 2 Ma) for samples C1 and C6 on Carnmenellis from the study of DARBYSHIRE and SHEPHERD (1985), but the whole-rock Rb-Sr isochron age (285 ± 19 Ma) has a large uncertainty. The $^{40}Ar/^{39}Ar$ cooling age of the Carn Marth granite is significantly younger than the Rb-Sr whole-rock age (298 ± 6 Ma) from DARBYSHIRE and SHEPHERD (1987). The Carn Marth pluton contains abundant xenocrysts of earlier granite, therefore the Rb-Sr age may reflect contamination from the earlier event.

Secondary muscovite taken from a stage 2 tourmaline-quartz vein from drill core (44) in the South Crofty Mine gives a $^{40}Ar/^{39}Ar$ plateau age of 286.6 ± 0.8 Ma, significantly younger than that for the magmatic muscovites in the Carnmenellis pluton (Table 3), but in excellent agreement with the inferred age for elvan emplacement in the South Crofty Mine and the cooling ages for the Carn Marth and Rosmanowas intrusives. Muscovite from a vein selvage in a base-metal pyroxene-garnet-bearing skarn intersected ~900 m

Table 3. $^{40}Ar/^{39}Ar$ Data

Sample #	Lithology	Mineral*	Total Gas Age	Plateau Age	Error (2σ)[&]	$\%^{39}Ar$ in plateau	Steps in plateau
Lands End							
Granites							
JTC-94-89	FGBGD	m	271.5	271.8	± 0.8	88.9	6
JTC-135-89	FGBG	m	272.1	272.3	± 0.9	91.1	6
JTC-136-89	CGBG	m	272.5	272.9	± 0.8	89.0	6
JTC-247-89	FGBGD	m	271.7	272.5	± 0.8	81.4	6
LE-E47625	CGBG	m	273.3	272.5	± 0.8	88.5	6
Mineralization							
JTC-107-89	GBV	m	269.9	270.4	± 0.9	92.4	4
JTC-129-89	GBV	m	267.2	268.4	± 0.8	88.6	5
JTC-147-89	GBV	m	270.0	270.5	± 0.8	88.8	6
JTC-177-89	GBV	m	272.4	272.3	± 0.8	84.5	6
Carnmenellis							
Granites							
JTC-57-89	CGBG/E	m	285.6	286.5	± 0.8	94.8	5
JTC-81-89	CGBG	b	289.9		± 0.9		
JTC-81-89	CGBG	m	290.5	290.7	± 0.9	89.4	6
JTC-83-89	CGBG/E	m	287.7	288.1	± 0.8	81.5	5
JTC-239-89	FGBGD	b	289.4		± 1.0		
JTC-239-89	FGBGD	m	288.5	288.7	± 0.8	88.9	6
JTC-242-89	CGBG	m	290.0	290.0	± 0.8	89.9	7
JTC-242-89	CGBG	b	290.0	292.1	± 1.0	75.2	3
JTC-243-89	CGBG	m	285.9	286.0	± 0.9	94.8	8
R2480	EBG	m	283.7	285.7	± 0.8	80.6	6
C5*	CGBG	m	288.7	289.2	± 0.8	85.8	7
C6*	CGBG	m	290.5	290.3	± 0.9	80.4	6
Mineralization							
JTC-44-89	GBV	m	285.2	286.6	± 0.8	86.4	6
JTC-80-89	GBV	m	280.7		± 0.9		
St. Austell							
Granites							
JTC-29-89	CLMG	b	277.4		± 0.9		
JTC-29-89	CLMG	m	276.7	276.9	± 0.8	92.0	8
JTC-30-89	CGBG	m	276.5	276.7	± 0.9	88.3	8
JTC-276-89	CGBG	b	277.8		± 1.0		
JTC-276-89	CGBG	m	278.1	278.3	± 0.8	90.2	7
JTC-289-89	FLMG	m	273.8	273.9	± 0.8	86.8	6
FG-1	FIG	m	267.1		± 0.9		
Mineralization							
JTC-284-89	GBV	m	270.4	270.3	± 0.8	70.6	5
G-5@	GBV	m	276.6	276.8	± 1.2	92.0	7
Bodmin Moor							
Granites							
JTC-312-89	CGBG	m	287.2	287.1	± 0.9	92.9	6
JTC-309-89	CGBG	m	288.2	288.1	± 0.8	86.6	6
Gunnislake							
JTC-200-89	CGBG	m	282.5	283.3	± 0.9	95.3	7
Mineralization							
JTC-197-89	GBV	m	280.7	283.1	± 0.9	53.8	4
Dartmoor							
Granites							
JTC-4-89	Fe-Skarn	hb	280.0	280.3	± 1.0	84.0	4
JTC-185-89	CGBG	m	270.5		± 0.8		
JTC-187-89	CGBG	m	271.0	271.5	± 0.8	95.0	5
JTC-188-89	CGBG	m	275.3	275.9	± 1.0	72.0	6
JTC-189-89	CMG	m	272.3		± 0.8		
Mineralization							
JTC-212-89	FGBGD	b	277.1		± 1.0		
Repeat 212-89			277.3		± 1.0		
Hemerdon							
Mineralization							
JTC-318E-89	SM	m	277.0	277.8	± 0.8	91.6	5
JTC-319C-89	GBV	m	286.2		± 0.9		

#CGBG=Coarse-grained biotite granite, FGBG=Fine-grained biotite-granite FGBGD=Fine-grained biotite-granite dike, CGBG/E=Coarse-grained biotite-granite near Elvan Contact, EBG=Equigranular biotite granite, CLMG=Coarse-grained Li-mica granite, FLMG=Fine-grained Li-mica granite, CMG=Coarse megacrystic granite, FIG=Fluorite Granite, SM=Secondary muscovite, GBV=Greisen bordered vein.

* m=muscovite, hb=hornblende, b=biotite; @ Snee, Unpublished Data;

&If no plateau age given error corresponds to the total gas age.

Table 4. Sm-Nd Data for Fluorite From Geevor Mine.

Sample	Sm (ppm)	Nd (ppm)	$\frac{^{147}Sm}{^{144}Nd}$	$\frac{^{143}Nd}{^{144}Nd}$	Error ($2\sigma \times 10^{-6}$)
D-Lode Geevor					
JTC-270-1a	25.3	129	0.1182	0.512139	(7)
JTC-270-2b	1.93	12.3	0.1578	0.512209	(8)
JTC-270-3c	0.819	2.515	0.1968	0.512273	(7)
JTC-270-4d	2.64	6.43	0.2484	0.512368	(8)

below the Wheal Jane Mine (6 km northeast of the Carnmenellis pluton), gives a total gas age of 280.7 ± 0.8 Ma, but shows an Ar loss profile with no plateau and therefore only represents a minimum age. An isochron plot of the oldest age spectrum steps yields a maximum age of 283.5 ± 0.3 Ma (2σ). Skarn-type mineralization is considered the earliest mineralization related to an intrusive event and should therefore define a minimum age for the intrusion. Fluorite Sm-Nd isochrons for the stage 3 mineralization in the South Crofty and Wheal Jane Mines define ages of 259 ± 7 Ma and 266 ± 3 Ma (2σ), respectively (CHESLEY et al., 1991). The stage 3 mineralization ages are in good agreement with fluid inclusion Rb-Sr isochron age of 269 ± 4 Ma (DARBYSHIRE and SHEPHERD, 1985) for a Sn-bearing quartz vein from the South Crofty mine. In the Wheal Jane mine, elvans clearly predate the emplacement of stage 3 mineralization (HOLL, 1988). At both South Crofty and Wheal Jane the age of main stage 3 mineralization clearly postdates the granite emplacement in the Carnmenellis region by 20 to 40 myrs and is significantly younger than any documented magmatism in the Cornubian batholith.

St. Austell Pluton

The St. Austell pluton contains multiple episodes of granite intrusions, the largest kaolin deposits in southwest England and is the only pluton to contain all of the minor granite phases as defined by EXLEY et al. (1983) and STONE and EXLEY (1985). Three monazite and three zircon fractions were analyzed from sample 276 of the main CGBG in the St. Austell pluton (Table 2; Fig. 2). A U-Pb analysis of one of the monazite splits is reversely discordant, but the $^{207}Pb/^{235}U$ age overlaps with the age of the other two concordant size fractions and all three give a weighted average $^{207}Pb/^{235}U$ age of 281.8 ± 0.4 Ma (2σ). The agreement in age from the different size fractions indicates that there is no inherited Pb. The zircon fractions were chosen on the basis of their euhedral form, pencil shape and clarity, all samples had a length to width ratio of between 5 to 10:1 suggesting the zircons probably grew from the granite melt. Data for all fractions are discordant, and judging from their $^{207}Pb/^{206}Pb$ ages of 307 to 292 Ma these fractions contain inherited Pb predating the St. Austell pluton. The $^{40}Ar/^{39}Ar$ data from sample 276 gives a plateau age of 278.3 ± 0.8 Ma, suggesting that the sample cooled to below the Ar closure temperature for muscovite within 3.5 myrs (~115°C myr^{-1}). Samples 29 and 30 are heavily altered CGBG and Li-mica granite from the Goonbarrow china clay pit and give indistinguishable plateau ages of 276.9 ± 0.8 Ma and 276.7 ± 0.9 Ma, respectively. Sample 29 is slightly younger than the unaltered CGBG granite in sample 276 and most likely represents protracted cooling or resetting caused by the intrusion of the younger Li-mica granite. Sample 289 is from the fine-grained biotite granite at the Wheal Martin deposit and gives a plateau-age of 273.9 ± 0.8 Ma, which appears to represent slower cooling or a younger magmatic event than the emplacement of either the Li-mica granite or the main CGBG. Muscovite from the fluorite granite (FG-1) yields a disturbed age spectrum and a total gas age of 267.7 ± 0.9 Ma. In thin section, the muscovite is ragged and appears to have reacted with later fluids to form interstitial fluorite, topaz, and secondary muscovite. The Ar-release spectrum appears to have two separate release plateaus containing 39% and 41% of the gas and may reflect a mixing of the two separate muscovite populations. Therefore, the muscovite total gas age only represents a minimum cooling age. The isochron for sample FG-1 yields an identical age for all points and a maximum age of 271.0 ± 0.4 Ma (2σ) using the oldest steps from the spectrum. The U-Pb ages are younger than previous estimates (285 to 301 Ma) for the age of emplacement of the main coarse-grained biotite St. Austell granite (HARDING and HAWKES, 1971; BRAY and SPOONER, 1983; DARBYSHIRE and SHEPHERD, 1985).

Sample G-5 is from a greisen-bordered vein in the Goonbarrow Pit, gives a $^{40}Ar/^{39}Ar$ plateau-age of 276.8 ± 1.2 Ma (2σ) (L. W. Snee, unpubl. data), and is in excellent agreement with the cooling age for the muscovite in the Goonbarrow Pit. Kaolinization is considered to be a younger, low-temperature process (SHEPPARD, 1977; BRISTOW and EXLEY, 1988); however, it appears to have little or no effect on the Ar systematics of the primary or secondary muscovites. Sample 284 is from the Wheal Remfry tourmaline breccia and yields a $^{40}Ar/^{39}Ar$ plateau-age of 270.3 ± 0.8 Ma. The Wheal Remfry breccia is a Sn-tourmaline breccia and postdates greisen vein mineralization on the basis of crosscutting relations (BRAY and SPOONER, 1983) and contains large inclusions of elvan material. The field relations and geochronology suggest elvan emplacement was no later than 270 Ma.

Bodmin Moor Pluton

Monazite from sample 312 is from the CGBG major granite phase of the Bodmin pluton and yields a $^{207}Pb/^{235}U$ age of 291.4 ± 0.8 Ma. The corresponding muscovite gives a plateau age of 287.1 ± 0.9 Ma and thus a cooling rate of 95°C myr^{-1}. The cooling age is in excellent agreement with sample 309 which yields a plateau age of 288.1 ± 0.8 Ma (Table 3). The $^{40}Ar/^{39}Ar$ ages are in excellent agreement with Rb-Sr biotite ages 287 ± 2 Ma (DARBYSHIRE and SHEPHERD, 1985); however, the Rb-Sr whole-rock age (275 ± 9 Ma) is in poor agreement with the U-Pb age.

Gunnislake Pluton

Gunnislake is a minor CGBG satellite intrusion located between the Bodmin Moor and the Dartmoor plutons and gives a $^{40}Ar/^{39}Ar$ plateau age of 283.1 ± 0.9 Ma for sample 200. Sample 197 is from a minor greisen bordered quartz vein in the Old Gunnislake mine and yields a plateau age of 283.2 ± 0.9 Ma, in excellent agreement with the muscovite cooling age of the intrusion.

Dartmoor Pluton

Two monazite samples were analyzed from quarries in the Dartmoor pluton which is the largest pluton in the batholith. Monazite samples 187 and 188 are both concordant and give $^{207}Pb/^{235}U$ ages of 278.2 ± 0.8 Ma and 280.4 ± 1.2 Ma, respectively. A hornblende (sample 4) from the metamorphic aureole of the Dartmoor pluton (2 km east of sample 188) gives a $^{40}Ar/^{39}Ar$ plateau age of 280.3 ± 1.0 Ma (Table 3; Fig. 3f), which is confirmed by an isochron analysis. The hornblende is from a garnet pyroxene hornblende magnetite skarn with fluid inclusion T_h = 350 to 475°C (SCRIVENER et al., 1987). Because of the high blocking temperature of hornblende, the $^{40}Ar/^{39}Ar$ age should also reflect the emplacement age of the granite and is in excellent agreement with the U-Pb age (280.4 ± 1.2 Ma). Corresponding muscovites from samples 187 and 188 yield plateau ages of 271.5 ± 0.8 Ma and 275.9 ± 1.0 Ma, respectively. An isochron plot of the latter at 275.7 ± 0.3 Ma (2σ) is in excellent agreement. These samples indicate cooling rates between ~60° and 85°C myr^{-1}. The difference in cooling rate between samples may reflect the location of sample 187 farther away from the pluton contact compared to sample 188. The cooling rates are also significantly slower than those of the other plutons and suggest the Dartmoor pluton may be exposed at a deeper level. The other two samples of muscovite (185, 189) exhibit disturbed age-spectra and give total gas ages of 270.5 ± 0.8 Ma and 272.3 ± 0.8 Ma. An isochron analysis of sample 185 yields an age of 276.2 ± 0.4 Ma which may yield a minimum cooling age. There are two generations of muscovite evident in thin section, one primary and the other secondary from the breakdown of primary muscovite, potassium-feldspar, and biotite and both age-spectra appear to have two separate pulses of gas release. The multiple emplacement ages and disturbed spectra are consistent with field relations which suggest that the Dartmoor pluton comprises several episodes of magmatism (BRAMMALL and HARWOOD, 1932; SCRIVENER, 1982). The U-Pb and $^{40}Ar/^{39}Ar$ ages are in excellent agreement with both the isotope dilution Rb-Sr whole-rock (280 ± 1 Ma) and mineral isochron ages (278 ± 2 Ma) from the same quarry as sample (188) of DARBYSHIRE and SHEPHERD (1985).

Hemerdon Pluton

Hemerdon is a small, highly altered, W-bearing satellite intrusion on the south flank of the Dartmoor batholith. The U-Pb data for a monazite from sample 318E of the Hemerdon granite is discordant (Fig. 2) and has a $^{207}Pb/^{206}Pb$ age of 298.3 ± 2.3 Ma (Table 2). This age is consistent with the older Rb-Sr whole-rock isochron age of 304 ± 23 Ma (DARBYSHIRE and SHEPHERD, 1987). However, due to the extensive hydrothermal alteration and potential for excess ^{230}Th in the monazite, both ages should be regarded with caution.

Samples 318E and 319C are from a drill core at the Hemerdon W-mine and both exhibit complete replacement of the coarse-grained biotite granite by secondary muscovite quartz and kaolinite. Sample 319C, a secondary muscovite from a greisen-bordered quartz vein, yields a total gas age of 286.2 ± 0.9 Ma and the age-spectrum exhibits an Ar loss profile (Fig. 3g) suggesting subsequent reheating. An isochron of the data gives a minimum age of 290.2 ± 0.4 Ma and should therefore be considered a minimum age and is consistent with the age for the Hemerdon pluton inferred from the monazite data. Sample 318E, a secondary muscovite from the Hemerdon granite, gives a plateau age of 277.8 ± 0.8 Ma (Table 3). This age is coincident with the time of emplacement and cooling of the neighboring Dartmoor pluton and may represent formation of secondary muscovite by high-temperature fluids and volatiles expelled during initial crystallization.

ORIGIN AND EMPLACEMENT OF THE CORNUBIAN BATHOLITH

Surprisingly, only a very limited amount of information is available on the time span over which granite magmas coalesce to form composite plutons and batholiths. The monazite and xenotime ages from this study clearly demonstrate that granite emplacement in the Cornubian batholith continued over a minimum of 25 myrs (Fig. 5). There is no apparent systematic relation between the age of a pluton and location within the batholith (Fig. 5). Furthermore, the individual plutons contain different intrusions that are resolvable with high-precision geochronology. The U-Pb ages give definitive evidence for magma emplacement over time spans of up to 4.5 myrs and the $^{40}Ar/^{39}Ar$ ages can be used to infer that emplacement and cooling of separate bodies within a pluton may have continued for as much as 10 myrs. These observations are in good agreement with the concept of composite plutons suggested by earlier workers (e.g., GHOSH, 1934; EXLEY and STONE, 1982). The longevity of silicic magma chambers has been modeled by HUPPERT and SPARKS (1988) and SPARKS et al. (1990). They suggested that magma bodies of a size similar to those of Cornwall would be expected to solidify within a period of less than 10^5 years. Therefore, the existence of composite intrusions with life spans of several million years requires repeated melting events (HUPPERT and SPARKS, 1988) or the existence of a deeper magmatic system that remained molten because of a continuous supply of heat from mantle-derived magmas (HALLIDAY et al., 1989; HALLIDAY, 1990).

The elvan dikes do not appear to be the result of separate magmatism that postdates major granitic intrusions as has been suggested (DARBYSHIRE and SHEPHERD, 1985; JACKSON et al., 1989; WILLIS-RICHARDS and JACKSON, 1989). The 286 Ma $^{40}Ar/^{39}Ar$ age inferred for the elvan emplacement at Carnmenellis, the 282 Ma age of the Wherry elvan (DARBYSHIRE and SHEPHERD, 1985) and the 270 Ma minimum age for the elvan at St. Austell suggest that elvan emplacement is probably coincident with major magmatism and that the ages depend on the location in the batholith. The data demonstrate that younger magmatism took place across the entire batholith. It is therefore conceivable that the emplacement of early plutons formed a barrier which prevented the younger granites from penetrating to the levels of the present-day surface. The elvans may represent dikes tapping into the upper portions of buried magmas shortly after emplacement, and they could possibly be feeders for contemporaneous felsic volcanism (DANGERFIELD and HAWKES, 1969).

There are three main schools of thought regarding the genesis of the granites of the Cornubian batholith. Several workers have suggested that melting was initiated in response to the crustal thickening by thin-skinned thrusting from the south during the Variscan orogeny (e.g., SHACKLETON et al., 1982; PEARCE et al., 1984). SHACKLETON et al. (1982) also pointed out that the crust in the region is too thin (<32 km) to generate the granites by melting in the zone where they now occur and suggested the granites were generated in the south, and injected to the north, along southward dipping structures as a single sheet-like granite mass with separate diapiric upwellings forming the exposed plutons. Other workers have suggested that the granites were derived from the mantle via fractional crystallization of a more mafic parent and crustal assimilation (e.g., SIMPSON et al., 1979; WATSON et al., 1984). A third possibility requires an elevated geothermal gradient, possibly due to basaltic underplating (HUPPERT and SPARKS, 1988), which resulted in regional melting of the lower crust (LEAT et al., 1987).

The ages presented here, together with a consideration of the chemistry and isotopic compositions of the granites (e.g., SHEPPARD, 1977; DARBYSHIRE and SHEPHERD, 1985, 1987) provide powerful constraints on the origin of the magmas. The first question to address is whether the batholith was a large interconnected reservoir or was built progressively from separate pulses of melting. The data presented here demonstrate unequivocally that the batholith was formed by the coalescing of separate granite intrusions over a >25 myr interval (Fig. 5). The absence of any relationship between the age of the plutons, their location in the batholith, and the duration of emplacement of both the batholith and the individual plutons are irreconcilable with models involving thin-skinned tectonics transporting magma from the south. A large interconnected magma system at shallow levels would be expected to crystallize in a short time span and not over the 25 myr period measured.

Models involving fractionation of mantle-derived magmas are difficult to reconcile with the large volume of highly fractionated granites in the batholith, the lack of more mafic endmembers and the high $\delta^{18}O$ and $^{87}Sr/^{86}Sr_i$ values (SHEPPARD, 1977; HAWKES and DANGERFIELD, 1978; DARBYSHIRE and SHEPHERD, 1985). We consider models involving crustal melting initiated by mantle-derived magmatism to be a more likely scenario; an elevated heat flux produced through underplating of basaltic magmas could account for semi-continuous granite magmatism over a >25 myr interval. MANNING and HILL (1990) suggested that the late topaz granites observed at St. Austell were the result of melting of refractory residue after partial melting and removal of the biotite-granite melt and are independent of fractional crystallization within the batholith. The timing of emplacement between the biotite-granites and the topaz granites would require a long-lived elevated heat source in the same area.

A more detailed evaluation of mechanisms of batholith formation requires discussion of the chemical composition for the granites and is beyond the scope of this paper. However, it is clear from the data presented here that the Cornubian batholith should be considered as a series of small anastomosing igneous bodies with each individual body having a discrete evolution after extraction from a comparable source, leading to a separate emplacement and cooling history.

COOLING HISTORY

The isotopic ages presented here provide not only evidence of protracted magmatism, but of a resolvable cooling history as defined by the difference between the $^{207}Pb/^{235}U$ monazite ($T_c \sim 725°C$) or xenotime ($T_c \sim 650°C$) ages and the $^{40}Ar/^{39}Ar$ muscovite ages ($T_c \sim 325°C$). In order to interpret the age differences of minerals rigorously, it is necessary to assess all of the uncertainties including the decay constants, spike calibration, and accepted age of the flux monitor (in the case of $^{40}Ar/^{39}Ar$) that could have introduced a systematic bias into either the U-Pb or $^{40}Ar/^{39}Ar$ results. Apart from the obvious use of internationally accepted values for the decay constants (STEIGER and JÄGER, 1977) and flux monitors (SAMSON and ALEXANDER, 1987), a further check is provided by the $^{40}Ar/^{39}Ar$ analysis of an amphibole from the Haytor skarn, in the aureole of the Dartmoor pluton. The amphibole yields a plateau age of 280.3 ± 1.0 Ma, in excellent agreement with the U-Pb monazite age of 280.4 ± 1.2 from a nearby granite sample (188). In addition, these ages are in good agreement with a whole-rock Rb-Sr age of 280 ± 1 Ma determined by isotope dilution for the Dartmoor pluton (DARBYSHIRE and SHEPHERD, 1985). Similarly, the $^{40}Ar/^{39}Ar$ muscovite ages are in excellent agreement with isotope dilution Rb-Sr biotite-isochron ages from the same localities in the plutons and on the same samples used in the original study of DARBYSHIRE and SHEPHERD (1985). The internal consistency of the $^{40}Ar/^{39}Ar$ method is observed in samples 242 and C6, which were both collected from the same quarry and yield ages of 290.0 ± 0.8 Ma and 290.3 ± 0.9 Ma, respectively.

Cooling times for the individual plutons, from emplacement down to the closure of muscovite to Ar, range between 1.9 and 6.7 myrs with a mean of 3.9 myrs ($\sim 100°C\ myr^{-1}$) (Fig. 6). These rates reflect the calculated times that elapsed between monazite and muscovite closure to diffusion; the actual cooling rate would initially be rapid, followed by slow asymptotic cooling towards an ambient value (e.g., NORTON and KNIGHT, 1977; CATHLES, 1981; HARRISON and MCDOUGALL, 1980). These cooling rates are much slower than those predicted by thermal modeling of cooling silicic magmas (SPERA, 1980; HUPPERT and SPARKS, 1988). Though there is no apparent correlation between cooling rate and age of a pluton, there appears to be a decrease in the overall cooling rate from Lands End in the southwest to Dartmoor in the northeast (Fig. 6).

Factors that could affect the granite cooling rates include: 1) initial magmatic temperature; 2) heat production of the granite; 3) thermal conductivity of the wall rocks; 4) mass of magma; 5) geometry of the granite body; 6) location of the sample within the pluton; 7) repeated igneous intrusion into the same area; 8) cooling from meteoric fluids; and 9) depth of emplacement. Because of the similar composition of the granites and country rocks across the area of the batholith, the initial temperature, heat production, and thermal

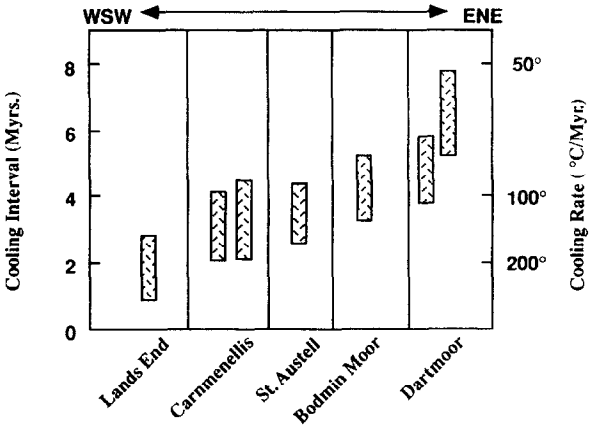

FIG. 6. Cooling interval of individual plutons within the Cornubian batholith. The cooling interval is defined as the difference in age between the closure of monazite to the diffusion of Pb (~725°C) and the closure of muscovite to Ar (~325°C).

conductivity of the wall rocks would be expected to produce only second-order effects. The presence of dikes, sheeted vein systems, and large roof pendants in the Lands End pluton indicates proximity to the upper portions of the pluton, while stable isotope analyses of fluid inclusions suggest interaction with meteoric fluids during early mineralization (JACKSON et al., 1982). Both factors would promote rapid cooling (e.g., SPERA, 1980, CATHLES, 1981). The Dartmoor pluton is the largest pluton in the batholith and contains several episodes of magmatism. The slow cooling rate (60° to 80°C myr^{-1}) disagrees with models of rapid cooling for the Dartmoor granite supposedly caused by rapid unroofing (WILLIS-RICHARDS and JACKSON, 1989). The sample locations are near the margins of the pluton and therefore would be expected to give maximum cooling rates. Gravity models of the batholith indicate a deep fault controlled trough just west of the Dartmoor pluton and a decrease in the estimated batholith thickness in the Dartmoor area (WILLIS-RICHARDS and JACKSON, 1989). The Dartmoor granite is characterized by coexisting very high salinity and dense vapor-rich fluid inclusions, consistent with fluids in equilibrium with a granite melt (RANKIN and ALDERTON, 1985). The same assemblages are also typical of the Birch Tor quartz-cassiterite tourmaline veins and greisen-bordered quartz veins of the Hemerdon mine of high-temperature magmatic-hydrothermal origin (SHEPHERD et al., 1985). In view of the S-deficient nature of the mineral assemblages, these observations strongly suggest that the Dartmoor mineralizing fluids were primarily magmatic and did not experience significant mixing with meteoric, sulfur-bearing fluids during emplacement and cooling. The long cooling history may also reflect heat loss primarily by conduction to the wall rocks and not due to heat loss from hydrothermal circulation.

There are few direct measurements of the cooling rates of plutons (from emplacement to ~300°C) to compare with the results of the present study. Most of the information and understanding of plutonic cooling rates are derived from quantitative modeling of igneous cooling by diffusive and convective heat transfer through porous media (e.g., JAEGER, 1964; NORTON and KNIGHT, 1977; NORTON and CATHLES, 1979; CATHLES, 1981, 1990; FURLONG et al., 1991). During initial intrusion, permeability will be very low, fluids will be unable to circulate and cooling will be primarily by conduction (NORTON, 1990; NORTON and CATHLES, 1979; CATHLES, 1981, 1990; FURLONG et al., 1991). As the magma crystallizes and fractures, fluids can circulate through the pluton in proportion to the extent of fracturing. In the presence of hydrothermal circulation, models have been used to suggest that cooling would be complete in as little as 10^3 to 10^5 years (SPERA, 1980; NORTON and CATHLES, 1979; CATHLES, 1981). Shortcomings of such models lie in the inability to incorporate multiple intrusive events and the effect of poorly known pluton geometry.

Modeling of the Carnmenellis pluton by WILLIS-RICHARDS and JACKSON (1989) in the absence of hydrothermal convection suggests that the upper portions of the pluton would cool rapidly, whereas the deeper portions of the pluton (>15 km) would remain molten after 15 to 20 myrs and would be a source for the mineralization and elvan dikes. Their model is based on geophysical estimates of the pluton shape and size and the assumption that the emplacement of the Carnmenellis pluton is as a single large magmatic body. In contrast, the field evidence (GHOSH, 1934), geochemistry (DARBYSHIRE and SHEPHERD, 1985, CHAROY, 1986), and geochronology support a multiple intrusive history. Hence, plutonism may be better represented as a series of successive smaller intrusions staggered in time, underneath and beside the main Carnmenellis granitic body. The depth of formation and geometry of these smaller plutons would dramatically influence their crystallization and cooling history by controlling the timing and extent of volatile exsolution, interaction with meteoric fluids, and contribute to the total heat budget of the system. The model of WILLIS-RICHARDS and JACKSON (1989) also fails to explain the lack of similar protracted cooling and mineralization histories for other plutons within the batholith and why major economic mineralization postdates the Carnmenellis pluton by 30 to 40 myrs.

MINERALIZATION

The overall mineralization history with respect to the Cornubian batholith lasted over 25 myrs (Fig. 5). However, the mineralization history for each pluton appears to be distinct. The stage 1 skarn mineralization age is in good agreement with the U-Pb emplacement age for the associated pluton as would be expected. Modeling of Sn-W-bearing fluid chemistry suggests that high-temperature, low f_{O_2} and low pH fluids are required for the transport of tin (e.g., HEINRICH, 1990; WILSON and EUGSTER, 1990). In addition, at low f_{O_2}, sulfur will partition more readily into the magma than into the exsolved aqueous phase (BURNHAM and OHMOTO, 1980), which is consistent with the sulfur-deficient nature of the stage 2 fluids. According to the models acidic Sn-bearing fluids expelled from the crystallizing magma will be buffered by the reaction:

$$3KAlSi_3O_8 + 2HCl = KAl_3Si_3O_{10}(OH)_2 + 6SiO_2 + 2KCl$$

and

$$3NaAlSi_3O_8 + 2HCl + KCl = KAl_3Si_3O_{10}(OH)_2 + 6SiO_2 + 3NaCl$$

forming secondary muscovite (e.g., HEINRICH, 1990). The age of stage 2 mineralization is best represented by $^{40}Ar/^{39}Ar$ secondary greisen-muscovite ages, and in the case of Bostraze and Goonbarrow agree within the limits of statistical resolution for the cooling ages of the plutonic muscovite. These ages define a minimum age for the first pulses of magmatic fluid and stage 2 mineralization during the initial crystallization and cooling of the pluton. In several cases, the secondary muscovite age is significantly younger than the cooling age of the host pluton (2–5 myrs), and may be correlated with a nearby magmatic event. The long cooling intervals for each pluton, with the exception of Lands End, suggest that meteoric fluids did not significantly interact with the plutons during emplacement and initial cooling.

The age of stage 3 mineralization is represented by the Sm-Nd fluorite-isochron ages and the Rb-Sr fluid inclusion age (269 ± 4 Ma; DARBYSHIRE and SHEPHERD, 1985). In the case of Carnmenellis stage 3 mineralization postdates magmatism by 25–40 myrs. Although some samples display an argon loss profile suggesting disturbance by a younger event. The secondary muscovite ages from stage 2 mineralization do not appear to record the age of the younger lower-temperature stage 3 fluids. The development of the stage 3 mineralization of similar age in the oldest (Carnmenellis) and youngest (Lands End) plutons suggest this was a regional event and not just centered on a single pluton. Stage 3 mineralizing fluids may thus reflect regional hydrothermal circulation driven by the elevated heat flux produced by the emplacement and crystallization of younger pulses of granite magmatism (<270 Ma), or fluid circulation driven by the elevated regional geotherm produced by the long-lived, multiply overlapping, plutonic episodes. Additional heat sources will certainly prolong the duration of fluid circulation such that the fluid flow would be realigned with respect to the new heat source (CATHLES, 1990; NORTON, 1990). Focusing of hydrothermal circulation by younger plutons may account for the asymmetric zoning of mineralization on the sides of the plutons.

CHRONOLOGY OF EVENTS

Integration of the geochronology with field relations and granite chemistry requires an emplacement and mineralization history that differs significantly from traditional views (e.g., STONE and EXLEY, 1985; DARBYSHIRE and SHEPHERD, 1985; JACKSON et al., 1989) and must involve long-lived multiple intrusive episodes, each with its own mineralization history but overlapping and overprinting earlier mineralizing events. The onset of major granitic magmatism in Cornwall began between 300 and 295 Ma (Fig. 7a). During cooling and crystallization of the magma, high-temperature magmatic fluids were released. A high geothermal gradient, emplacement of younger granite magmas and slow cooling served to prevent external fluids from entering the system (Fig. 7a). Major granitic intrusion continued in different regions of the batholith from ~295 Ma to ~275 Ma (Fig. 7b). Emplacement of elvan dikes was coincident with magmatism and continued to at least 270 Ma. Formation of stage 1 skarn mineralization was directly related to the timing of intrusion.

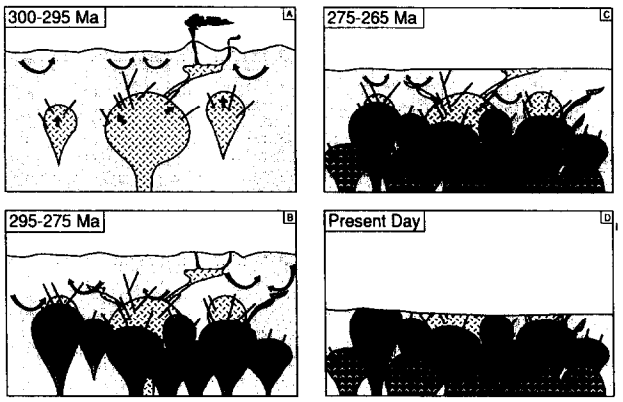

FIG. 7. Schematic illustration depicting the emplacement history of the plutons in the Cornubian batholith and relationship to mineralization. (A) Early emplacement of granite intrusions within the Cornubian batholith; (B) Emplacement of the bulk of the exposed Cornubian batholith from ~295 Ma down to ~275 Ma; (C) Emplacement of chemically specialized granites; unexposed granite intrusions and stage-III mineralization; see text for detailed explanation.

Further cooling of the granites and expulsion of magmatic fluids continued, with the location of fractures and deposition of stage 2 mineralization controlled by the pattern of preexisting fractures and the regional tectonic framework. Between 275 and 265 Ma the chemically specialized granites and late elvans were emplaced, and the magmatic fluid system collapsed allowing external fluids into the upper portions of the plutons (Fig. 7c). Circulation of external fluids leached metals and sulfur from the country rocks and plutons. These fluids mixed with the late magmatic fluids expelled from the buried crystallizing magmas initiating stage 3 mineralization. Continued circulation of external fluids was driven by the elevated regional geothermal gradient and latent heat of crystallization derived from deeper magmatism. Deposition of stage 3 hydrothermal mineralization was controlled by preexisting fractures and by overpressuring leading to hydrofracturing, rupture, mineral deposition, and resealing of the system. Stage 4 mineralization commenced after the emplacement and cooling of the batholith was completed and was triggered by a change in the regional tectonic stresses (e.g., SHEPHERD and SCRIVENER, 1987).

DISCUSSION

The lack of available high-precision geochronologic investigations of ore deposition make extension of this model to other tin deposits, much less other granite-related hydrothermal ore deposits, somewhat tenuous. However, several important observations should be made. The multiple intrusive nature of granite batholiths are well documented (e.g., PITCHER et al., 1985), and supporting evidence exists that many plutons are composed of discrete lithologic units distinguishable in age (e.g., GEISSMAN et al., 1992); however, the shape and size of individual intrusions is often poorly known. The spatial and temporal multiplicity of the magmas will lend itself to independent crystallization, fluid expulsion, fluid mixing, and mineral deposition histories.

Recent two-dimensional models have been used to sim-

ulate the temporal and spatial variations in the geothermal gradient of regions where the distribution and rates of emplacement of igneous heat sources are important (BARTON and HANSON, 1989; HANSON and BARTON, 1989). Such models have been used to demonstrate that the background geothermal gradients between intrusions may be elevated by 5° to 30°C km^{-1}, and depending on the abundance, depth of emplacement and timing of subsequent intrusions can remain elevated for significant time intervals (several tens of millions of years) before returning to normal geothermal gradients.

The existence of large regional hydrothermal circulation systems associated with the emplacement of granite batholiths (e.g., TAYLOR, 1978; CRISS and TAYLOR, 1983) and regional metamorphism (e.g., WOOD and WALTHER, 1986; FERRY and DIPPLE, 1991) is well documented. The exact conditions that permit these large circulation systems and the timing of fluid flow with regard to the emplacement and cooling of the batholiths are poorly understood. The presence of long-lived geothermal anomalies and large-scale fluid circulation that could be modified depending on the relation and timing of subsequent intrusions is conducive to long-lived mineral deposition. The amount and size of subsequent magmatism and the degree by which late hydrothermal flow is realigned and concentrated in pre-existing fractures may help determine the economic viability of an area.

The sequences of mineralizing events in tin deposits around the world is strikingly similar despite the significant variations in depositional environment. Mineralization is restricted roughly to four main paragenetic sequences (e.g., KELLY and RYE, 1979; PATTERSON, 1981; KWAK, 1987; SILLITOE et al., 1975): (1) endo- and exo-skarn mineralization; (2) a high-temperature, sulfur-deficient Sn + W bearing oxide + silicate stage; (3) a lower temperature base metal (Cu, Pb, Zn ± Sn) bearing sulfide + silicate + fluorite stage and (4) a late low-temperature base metal sulfide + carbonate + barite. Multiple overlapping mineralization episodes are often distinguished within a sequence. Stable isotope and fluid inclusion studies have convincingly demonstrated that the early high-temperature fluids are of magmatic derivation. In contrast, mineralization during the later sequences is dominated by meteoric (non-magmatic) fluids, with different degrees of mixing in between (e.g., PATTERSON, 1981; SUN and EADINGTON, 1987; TAYLOR, 1979).

It is only with recent geochronological methods that we have been able to resolve not only the differences in time between the different paragenetic sequences, but within an individual sequence. These time differences cannot be explained by simple cooling and collapse of a single pluton-driven hydrothermal system.

Acknowledgments—We wish to thank M. Owen, P. Gribble, and S. Speed of Carnon Consolidated Limited for access to the South Crofty and Wheal Jane Mines, M. Mount and A. Reynolds of Geevor Mining Ltd. for access to the Geevor Mine, B. Cooper for access to the Haytor Fe- Mine and C. Bristow of English China Clay International Ltd. for access to E.C.C. properties and for useful discussion and geologic expertise during sample collection. C. Smale and H. Bell (deceased) provided samples FG-1 and G-5, respectively. F. Darbyshire kindly provided the samples used in her original study, unpublished data and useful discussion with respect to her Rb-Sr analyses. JTC would like to thank S. Harlan and R. Yeoman who ran the day shift for $^{40}Ar/^{39}Ar$ analysis at the U.S. Geological Survey in Denver. The work presented represents a portion of the senior author's Ph.D dissertation at the University of Michigan. This research was supported by National Science Foundation grants EAR 8616061, 8804072 and 9004413 to A.N.H. and by the Denver U.S. Geological Survey $^{40}Ar/^{39}Ar$ Geochronology project. We are indebted to W. Kelly, S. Kesler, J. O'Neil, J. Mauk, M. Ohr, A. Arribas, A. Goode and M. Miller for discussion and/or critical review of the original manuscript. This paper is published with the approval of the Director of the British Geological Survey (NERC) and the Director of the U.S. Geological Survey. Thoughtful reviews for *GCA* by K. Ludwig, H. Stein, J. Ruiz, and I. Fanning greatly improved the manuscript.

Editorial handling: K. R. Ludwig

REFERENCES

ALDERTON D. H. M. (1975) Fluid inclusion studies in SW England. *Ussher Soc. Proc.* **3**, 214–217.

ALDERTON D. H. M. (1978) Fluid inclusion data for lead-zinc ores from SW England. *Inst. Mining Metallurgy Trans.* **87**, 132–135.

BARTON M. D. and HANSON R. B. (1989) Magmatism and the development of low pressure metamorphic belts: Implications from the western United States and thermal modeling. *Geol. Soc. Amer. Bull.* **101**, 1051–1065.

BRAMMALL A. and HARWOOD H. F. (1932) The Dartmoor granites. *J. Geol. Soc. London* **88**, 171–237.

BRAY C. J. and SPOONER E. T. C. (1983) Sheeted vein Sn-W mineralization and greisenization associated with economic kaolinization, Goonbarrow China Clay Pit, St. Austell, Cornwall, England: Geologic relationships and geochronology. *Econ. Geol.* **78**, 1064–1089.

BRISTOW C. M. and EXLEY C. S. (1988) Kaolin Deposits of the United Kingdom. Internal Report English China Clay Int.

BURNHAM C. W. and OHMOTO H. (1980) Late-stage processes of felsic magmatism. In *Granitic Magmatism and Related Mineralization* (ed. S. ISHIHARA and S. TAKENOUCHI) *The Society of Mining Geologists of Japan, Mining Geology Special Issue* **8**. 1–11.

CATHLES L. M. (1981) Fluid flow and genesis of hydrothermal ore deposits. *Econ. Geol.* (75th Anniv. Vol), 424–457.

CATHLES L. M. (1990) Scales and effects of fluid flow in the upper crust. *Science* **248**, 323–329.

CHAPPELL B. W. and WHITE A. J. (1974) Two contrasting granite types. *Pacific Geology* **8**, 173–174.

CHAROY B. (1986) The genesis of the Cornubian batholith (southwest England): The example of the Carnmenellis pluton. *J. Petrol.* **27**, 571–604.

CHESLEY J. T., HALLIDAY A. N., and SCRIVENER R. C. (1991) Samarium-neodymium direct dating of fluorite mineralization. *Science* **252**, 949–951.

COPELAND P., PARRISH R. R., and HARRISON T. M. (1988) Identification of inherited radiogenic Pb in monazite and implications for U-Pb systematics. *Nature* **333**, 760–763.

CRISS R. E. and TAYLOR H. P. (1983) An $^{18}O/^{16}O$ and D/H study of tertiary hydrothermal systems in the southern half of the Idaho batholith. *Geol. Soc. Amer. Bull.* **94**, 640–663.

DALRYMPLE G. B. and LANPHERE M. A. (1969) *Potassium-Argon Dating*. Freeman.

DALRYMPLE G. B. and LANPHERE M. A. (1974) $^{40}Ar/^{39}Ar$ age spectra of some undisturbed terrestrial samples. *Geochim. Cosmochim. Acta* **38**, 715–738.

DALRYMPLE G. B., ALEXANDER E. C., LANPHERE M. A., and KRAKER G. P. (1981) Irradiation of samples for $^{40}Ar/^{39}Ar$ dating using the Geologic Survey TRIGA reactor. *USGS Prof. Paper* **1176**.

DANGERFIELD J. and HAWKES J. (1969) Unroofing of the Dartmoor granite and possible consequences with regard to mineralization. *Ussher Soc. Proc.* **3**, 122–131.

DARBYSHIRE D. P. F. and SHEPHERD T. J. (1985) Chronology of granite magmatism and associated mineralization, SW England. *J. Geol. Soc. London* **142,** 1159–1178.

DARBYSHIRE D. P. F. and SHEPHERD T. J. (1987) Chronology of magmatism in southwest England: The minor intrusions. *Ussher Soc. Proc.* **4,** 431–438.

DAVISON E. H. (1927) Recent evidence regarding the zonal arrangement of minerals in the Cornish Lodes. *Econ. Geol.* **22,** 475–479.

DE LA BECHE H. T. (1839) *Report on the Geology of Cornwall, Devon and West Somerset.* British Geol. Survey Mem.

DINES H. G. (1956) *The Metalliferous Mining Region of Southwest England.* British Geol. Survey Mem.

DODSON M. H. (1973) Closure temperature in cooling geochronological and petrological systems. *Contrib. Mineral. Petrol.* **40,** 259–274.

DURRANCE E. H., BROMLEY A. V., BRISTOW C. M., HEATH M. J., and PENMAN J. M. (1982) Hydrothermal circulation and post-magmatic changes in the granites of southwest England. *Ussher Soc. Proc.* **5,** 304–319.

EDMONDS E. A., MCKEOWN M. C., and WILLIAMS M. (1969) *South-West England.* Her Majesty's Stationary Office.

EXLEY C. S. and STONE M. (1982) Hercynian intrusive rocks, In *Intrusive Rocks of the British Isles.* (ed. D. S. SUTHERLAND), pp. 287–320. Wiley.

EXLEY C. S., STONE M., and FLOYD P. A. (1983) Composition and petrogenesis of the Cornubian granite batholith and post-orogenic volcanic rocks in Southwest England. In *The Variscan Fold Belt in the British Isles* (ed. P. L. HANCOCK), pp. 153–177. Adam Hilger Ltd.

FERRY J. M. and DIPPLE G. M. (1991) Fluid flow, mineral interactions and metasomatism. *Geology* **19,** 211–214.

FLECK R. J., SUTTER J. F., and ELLIOT D. H. (1977) Interpretation of discordant $^{40}Ar/^{39}Ar$ age-spectra of Mesozoic tholeiites from Antarctica. *Geochim. Cosmochim. Acta* **41,** 15–32.

FURLONG K. P., HANSON R. B., and BOWERS J. R. (1991) Modeling thermal regimes. In *Short Course on Contact Metamorphism* (ed. D. M. KERRICK) pp. 437–505. Geologic Society of America **26.**

GARNETT R. H. T. (1965) Local mineral zoning in Geevor tin mine, Cornwall. *Czechoslovakia Geol. Survey* **1,** 91–96.

GANGULY J. and RUIZ J. (1987) Time-temperature relation of mineral isochrons: A thermodynamic model and illustrative examples for the Rb-Sr system. *Earth Planet. Sci. Lett.* **81,** 338–348.

GEISSMAN J. W., SNEE L. W., GRAASKAMP G. W., CARTEN R. B., and GERAGHTY E. P. (1992) Deformation and age of the Red Mountain intrusive system (Urad-Henderson molybdenum deposits), Colorado: Evidence from paleomagnetic and $^{40}Ar/^{39}Ar$ data. *GSA Bull.* **104,** 1031–1047.

GHOSH P. K. (1934) The Carnmenellis granite: Its petrology, metamorphism and tectonics. *J. Geol. Soc. London* **90,** 240–276.

HALLIDAY A. N. (1980) The timing of early and main stage ore mineralisation in SW Cornwall. *Econ. Geol.* **75,** 752–759.

HALLIDAY A. N. (1990) Reply to comment of R. J. S. Sparks and H. E. Huppert and C. J. N. Wilson. *Earth Planet. Sci. Lett.* **99,** 390–394.

HALLIDAY A. N., MAHOOD G. A., HOLDEN P., METZ J. M., DEMPSTER T. J., and DAVIDSON J. P. (1989) Evidence for long residence times of rhyolitic magma in the Long Valley magmatic system: The isotopic record in precaldera lavas of Glass Mountain. *Earth Planet. Sci. Lett.* **94,** 274–290.

HAMPTON C. M. and TAYLOR P. N. (1983) The age and nature of the basement in southern Britain: Evidence from Sr and Pb isotopes in granite. *J. Geol. Soc. London* **140,** 499–509.

HANSON R. B. and BARTON M. D. (1989) Thermal development of low pressure metamorphic belts: Results from 2-dimensional numerical models. *J. Geophys. Res.* **94,** 10363–10377.

HARDING R. R. and HAWKES J. R. (1971) The Rb-Sr age and K-Rb ratios of samples from the St Austell granite, Cornwall. *Inst. Geol. Sci. Rept.* **71/6.**

HARRISON T. M. (1981) Diffusion of ^{40}Ar in hornblende. *Contrib. Mineral. Petrol.* **78,** 324–331.

HARRISON T. M. and MCDOUGALL I. (1980) Investigations of an intrusive contact northwest Nelson, New Zealand-I: Thermal, chronological and isotope constraints. *Geochim. Cosmochim. Acta.* **44,** 1985–2003.

HAWKES J. R. and DANGERFIELD J. (1978) The Variscan granites of southwest England: A progress report. *Ussher Soc. Proc.* **4,** 158–171.

HEAMAN L. and PARRISH R. R. (1991) U-Pb geochronology of accessory minerals. In *Applications of Radiogenic Isotope Systems to Problems in Geology,* (ed. L. HEAMAN and J. N. LUDDEN), pp. 59–100 *Mineralogical Association of Canada* **19.**

HEINRICH C. A. (1990) The chemistry of hydrothermal tin (tungsten) ore deposition. *Econ. Geol.* **85,** 457–481.

HILL P. I. and MANNING D. A. C. (1987) Multiple intrusions and pervasive hydrothermal circulation in the St Austell granite, Cornwall. *Ussher Soc. Proc.* **6,** 447–453.

HILL J. B. and MACALISTER D. A. (1906) Geology of Falmouth and Truro and of the mining districts of Camborne and Redruth. *Mem. Geol. Surv. Great Brit.* **352** 64.

HOLL C. J. (1988) Mineralization at the Wheal Jane Mine. M.Sc. thesis, Camborne School of Mines, England.

HUPPERT H. E. and SPARKS R. S. J. (1988) The generation of granitic magmas by intrusion of basalt into continental crust. *J. Petrol.* **29,** 599–624.

JACKSON N. J. (1977) The geology and mineralization of the St. Just Mining district, west Cornwall. Ph.D. thesis, London University.

JACKSON N. J., HALLIDAY A. N., SHEPPARD S. M. F., and MITCHELL J. G. (1982) Hydrothermal activity in the St. Just mining district, Cornwall, England. In *Metallization Associated with Acid Magmatism* (ed. A. M. EVANS) pp. 137–139. Wiley.

JACKSON N. J., WILLIS-RICHARDS J., MANNING D. A. C., and SAMS M. S. (1989) Evolution of the Cornubian ore field, southwest England: Part II. Mineral deposits and ore-forming processes. *Econ. Geol.* **84,** 1101–1133.

JAEGER J. C. (1964) Thermal effects of intrusions. *Rev. Geophys.* **2,** 443–466.

KELLY W. C. and RYE R. O. (1979) Geologic, fluid inclusion, and stable isotope studies of the tin-tungsten deposits of Panasqueira, Portugal. *Econ. Geol.* **74,** 1721–1819.

KERRICK D. M. (1990) The Al_2SiO_4 polymorphs. In *Rev. Mineral. 22* (ed. P. H. RIBBE), pp. 353–361. Mineral. Soc. Amer.

KWAK T. A. P. (1987) *W-Sn Skarn Deposits and Related Metamorphic Skarns and Granatoids.* Elseveir.

LEAT P. T., THOMPSON R. N., MORRISON M. A., HENDRY G. L., and TRAYHORN S. C. (1987) Geodynamic significance of post Variscan intrusive and extrusive potassic magmatism in southwest England. *Royal Soc. Edinburgh Trans.* **77,** 349–360.

LUDWIG K. R. (1991) ISOPLOT: A plotting and regression program for radiogenic-isotope data. *U.S. Geol. Survey Open File Rept.* **9.**

MANHES G., ALLEGRE C. J., and PROVOST A. (1984) U-Th-Pb systematics of the eucrite "Juvines": Precise age determination of evidence for exotic lead. *Geochim. Cosmochim. Acta* **48,** 2247–2264.

MANNING D. A. C. and HILL P. I. (1990) The petrogenic and metallogenic significance of topaz granites from SW England orefield. *GSA Spec. Paper* **246,** 364–371.

MATTINSON J. M. (1986) Geochronology of high pressure-low temperature Franciscan metabasites: A new approach using the U-Pb system. *GSA Mem.* **164,** 95–105.

MCDOUGALL I. and HARRISON T. M. (1988) *Geochronology and Thermochronology by the $^{40}Ar/^{39}Ar$ Method.* Oxford Press.

MILLER C. F., STODDARD E. F., BRADFISH L. J., and DOLLASE W. E. (1981) Composition of plutonic muscovite: Genetic implications. *Canadian Mineral.* **19,** 25–34.

MOUNT M. (1985) Geevor Mine: A review. In *High Heat Production (HHP) Granites, Hydrothermal Circulation, and Ore Genesis,* pp. 221–238. The Inst. of Mining and Mettalurgy.

NESBITT B. E. (1990) Fluid flow and chemical evolution in the genesis of hydrothermal ore deposits. In *Short Course on Fluids in Tectonically Active Regimes of the Continental Crust* (ed. B. E. NESBITT), pp. 261–292. *Mineral. Assoc. Canada.*

NORTON D. (1990) Pore fluid pressures near magma chambers. In *The Role of Fluids in Crustal Processes,* (ed. J. D. BREDEHOEFT and D. NORTON), pp. 42–49. National Academy Press.

NORTON D. and CATHLES L. M. (1979) Thermal aspects of ore deposition. In *Geochemistry of Hydrothermal Ore Deposits*, 2d. ed. (ed. H. L. BARNES), pp. 611–631. Wiley & Sons.

NORTON D. and KNIGHT J. (1977) Transport phenomena in hydrothermal systems: Cooling plutons. *Amer. J. Sci.* **277**, 937–981.

NORTON D. and TAYLOR H. P., JR. (1979) Quantitative simulation of the hydrothermal systems of crystallizing magmas on the basis of transport and oxygen isotope data: An analysis of the Skaergaard intrusion. *J. Petrol.* **20**, 421–486.

PARRISH R. R. (1990) U-Pb dating of monazite and its application to geological problems. *Canadian J. Earth Sci.* **27**, 1431–1450.

PARRISH R. R., RODDICK J. C., LOVERIDGE W. D., and SULLIVAN R. W. (1987) Uranium-lead analytical techniques at the geochronological laboratory, Geological Survey of Canada. In *Radiogenic Age and Isotopic Studies: Report 1; Geological Survey of Canada Paper 87-2*, pp. 3–7.

PATTERSON D. J. (1981) Geologic setting and genesis of the cassiterite-sulfide mineralization at Renison Bell, western Tasmania. *Econ. Geol.* **76**, 393–438.

PEARCE J. A., HARRIS N. B. W., and TINDLE A. G. (1984) Trace element discrimination diagrams for the tectonic interpretation of granitic rocks. *J. Petrol.* **25**, 956–983.

PITCHER W. S., ATHERTON M. P., COBBING E. J., and BECKINSALE R. D. (1985) *Magmatism at the Plate Edge: The Peruvian Andes.* Blackie Halsted Press.

PRYCE W. (1778) *Mineralogia Cornubiensis.* Barton Ltd.

RANKIN A. H. and ALDERTON D. H. M. (1985) Chemistry and evolution of hydrothermal fluids associated with the granites of southwest England. In *High Heat Production (HHP) Granites, Hydrothermal Circulation and Ore Genesis*, pp. 287–300. The Inst. of Mining and Metallurgy.

REID C. and FLETT J. S. (1907) The geology of the Lands End District. *Mem. Geol. Surv. Great Brit.* **351.**

RODDICK J. C., CLIFF R. A., and REX D. C. (1980) The evolution of excess argon in Alpine biotites-A $^{40}Ar/^{39}Ar$ analysis. *Earth Planet. Sci. Lett.* **48**, 185–208.

SAMSON S. D. and ALEXANDER E. C. (1987) Calibration of the interlaboratory $^{40}Ar/^{39}Ar$ dating standard, MMhb-1. *Chem. Geol.* **66**, 27–34.

SCHÄRER U. (1984) The effect of initial ^{230}Th disequilibrium on young U-Pb ages: The Makalu case, Himalayas. *Earth Planet. Sci. Lett.* **67**, 191–204.

SCRIVENER R. C. (1982) Tin and related mineralization of the Dartmoor granite. Unpub. Ph.D. thesis, Univ. of Exeter.

SCRIVENER R. C., COOPER B. V., and GEORGE M. C. (1987) Mineralogy and paragenesis of the Haytor iron deposit. *Ussher Soc. Proc.* **6**, 558.

SHACKLETON R. M., RIES A. C., and COWARD M. P. (1982) An interpretation of the Variscan structures in SW England. *J. Geol. Soc. London* **139**, 533–541.

SHEPPARD S. M. F. (1977) The Cornubian batholith, southwest England: D/H and $^{18}O/^{16}O$ studies of kaolinite and other alteration minerals. *J. Geol. Soc. London* **133**, 573–591.

SHEPHERD T. J. and SCRIVENER R. C. (1987) Role of basinal brines in the genesis of polymetallic vein deposits, Kit Hill-Gunnislake area, SW England. *Ussher Soc. Proc.* **6**, 491–497.

SHEPHERD T. J., MILLER M. F., SCRIVENER R. C., and DARBYSHIRE D. P. F. (1985) Hydrothermal fluid evolution in relation to mineralization in southwest England with special reference to the Dartmoor-Bodmin area. In *High Heat Production (HHP) Granites, Hydrothermal Circulation and Ore Genesis.* pp. 345–364. The Inst. of Mining and Metallurgy.

SILLITOE R. H., HALLS C., and GRANT J. N. (1975) Porphyry tin deposits in Bolivia. *Econ. Geol.* **70**, 913–927.

SIMPSON P. R., BROWN G. C., PLANT J., and OSTLE D. (1979) Uranium mineralization and granite magmatism in the British Isles. *Royal Soc. London Phil. Trans.* **A29**, 385–412.

SKINNER B. J. (1979) The many origins of hydrothermal mineral deposits. In *Geochemistry of Hydrothermal Ore Deposits*, 2d. ed. (ed. H. L. BARNES), pp. 1–21. Wiley & Sons.

SNEE L. W. (1982) Emplacement and cooling of the Pioneer batholith, southwestern Montana. Ph.D. thesis, Ohio State Univ.

SNEE L. W., SUTTER J. F., and KELLY W. C. (1988) Thermochronology of economic mineral deposits: Dating the stages of mineralization at Panasqueira, Portugal by high precision $^{40}Ar/^{39}Ar$ age-spectrum techniques on muscovite. *Econ. Geol.* **83**, 335–354.

SPARKS R. S. J., HUPPERT H. E., and WILSON C. J. N. (1990) Comment on "Evidence for long residence times of rhyolitic magma in the Long Valley magmatic system: The isotopic record in precaldera lavas of Glass Mountain" by A. N. HALLIDAY, G. A. MAHOOD, P. HOLDEN, J. M. METZ, T. J. DEMPSTER, and J. P. DAVIDSON. *Earth Planet. Sci. Lett.* **99**, 387–390.

SPERA F. (1980) Thermal evolution of plutons: A parameterized approach. *Science* **207**, 299–301.

STEIGER E. H. and JÄGER E. (1977) Subcommission on geochronology, convention on the use of decay constants in geo- and cosmochronology. *Earth Planet. Sci. Lett.* **36**, 359–362.

STONE M. and EXLEY C. S. (1985) High heat production granites of southwest England and their associated mineralization: A review. In *High Heat Production (HHP) Granites, Hydrothermal Circulation and Ore Genesis*, pp. 571–593. The Inst. of Mining and Metallurgy.

SUN S. and EADINGTON P. J. (1987) Oxygen isotope evidence for the mixing of magmatic and meteoric waters during tin mineralization in the Mole Granite, New South Wales, Australia. *Econ. Geol.* **82**, 43–52.

TAYLOR H. P. (1978) Oxygen and hydrogen isotope studies of plutonic granite rocks. *Earth Planet. Sci. Lett.* **38**, 177–210.

TAYLOR H. P. (1979) Oxygen and hydrogen isotope relationships in hydrothermal mineral deposits. In *Geochemistry of Hydrothermal Ore Deposits*, 2d. ed. (ed. H. L. BARNES), pp. 236–277. Wiley & Sons.

TAYLOR R. G. (1969) *Geology of Tin Deposits.* Elsevier.

TILTON G. R. T. (1973) Isotopic lead ages of chondritic meteorites. *Earth Planet. Sci. Lett.* **19**, 321–329.

VAN MARCKE DE LUMMEN G. and VERKAEREN J. (1985) Mineralogic observations and genetic considerations relating to skarn formation at Botallack, Cornwall, England. In *High Heat Production (HHP) Granites, Hydrothermal Circulation and Ore Genesis.* The Inst. of Mining and Metallurgy, London, 535–548.

WATSON J. V., FOWLER M. B., PLANT J. A., and SIMPSON P. R. (1984) Variscan-Caledonian comparisons: Late orogenic granites. *Ussher Soc. Proc.* **6**, 2–12.

WHITE D. E. and HEROPOULOS C. (1986) Active and fossil hydrothermal convective systems of the Great Basin. *Geotherm. Res. Council Special Report* **13**, 41–53.

WILLIS-RICHARDS J. and JACKSON N. J. (1989) Evolution of the Cornubian ore field: Part I. Batholith modeling and ore distribution. *Econ. Geol.* **84**, 1078–1100.

WILSON G. A. and EUGSTER H. P. (1990) Cassiterite solubility and tin speciation in supercritical chloride solutions. In *Fluid-Mineral Interactions: A tribute to H. P. Eugster* (ed. R. J. SPENCER and I-MING CHOU), *The Geochem. Soc. Spec. Pub.* **2**, 179–197.

WOOD B. J. and WALTHER J. V. (1986) Fluid flow during metamorphism and its implication for fluid rock ratios. In *Fluid-Rock Interactions During Metamorphism* (ed. J. V. WALTHER and B. J. WOOD), pp. 109–131. Springer-Verlag.

YORK D. (1969) Least squares fitting of a straight line with correlated errors. *Earth Planet. Sci. Lett.* **5**, 320–324.

APPENDIX I

Sample #	Location	Sample Description	Grid Reference
Lands End			
Granites			
JTC-94-89	Geevor Mine15 W 4 Crosscut.	FGBG dike in metamorphic aureole.	SW 375 345
JTC-135-89	Castle-an-Dinas Quarry.	FGBG	SW 489 344
JTC-136-89	New Mill Quarry.	CGBG	SW 459 342
JTC-247-89	Robins Rocks at Porthmeor Pt.	FGBG dike in metamorphic aureole.	SW 425 380
LE-E47625*	Rosewall Hill Quarry.	CGBG	SW 497 391
Mineralization			
JTC-107-89	Geevor Mine 14 level.	GBV in CGBG wallrock, Simms lode.	SW 375 345
JTC-129-89	Geevor Mine 15 level.	GBV in FGBG wallrock, Corenation lode.	"
JTC-147-89	Geevor Mine 15 level.	GBV in CGBG wallrock, Coronation lode.	"
JTC-177-89	Bostraze China Clay Pit.	GBV in CGBG wallrock.	SW 385 315
Carnmenellis			
Granites			
JTC-57-89	South Crofty 360 Sub-level.	CGBG at elvan contact.	SW 675 411
JTC-81-89	Bosahan Quarry.	CGBG	SW 730 301
JTC-81-89	"	"	"
JTC-83-89	South Crofty 310 level.	CGBG 3.5 m from elvan.	SW 675 411
JTC-239-89	Pen Ryn Quarry.	FGBG dike.	SW 737 332
JTC-239-89	"	"	SW 737 332
JTC-242-89	Pen Ryn Quarry.	CGBG	SW 737 332
JTC-242-89	"	"	SW 737 332
JTC-243-89	Abandoned Quarry on Carn Marth.	CGBG	SW 720 410
R2480*	Rosemanawas Quarry Deep Bore Hole.	EBG	SW 736 347
C5-FD*	Carnsew Quarry.	CGBG	SW 758 345
C6-FD*	Pen Ryn Quarry.	CGBG	SW 737 332
Mineralization			
JTC-44-89	South Crofty 380 level.	In drill core 91 m between 4 and 8 lodes.	SW 675 411
JTC-80-89	Wheal Jane Deep Bore Hole.	Base metal-bearing skarn in drill hole.	SW 775 425
St. Austell			
Granites			
JTC-29-89	Goonbarrow Pit.	Li Mica Granite	SX 005 570
JTC-29-89	"	"	"
JTC-30-89	"	CGBG	"
JTC-276-89	Luxulyan Quarry.	CGBG	SX 053 591
JTC-276-89	"	CGBG	"
JTC-289-89	Wheal Martyn.	FGBG	SW 995 555
FG-1***	Goonvean and Rostowrack.	Hard purple FIG.	SW 940 555
Mineralization			
JTC-284-89	Wheal Remfry Breccia.	Tourmaline breccia.	SW 925 975
G-5**	Goonbarrow Pit.	Greisen bordered vein.	SX 005 570
Bodmin Moor			
Granites			
JTC-309-89	DeLank Quarries-St. Breward.	CGBG	SX 101 755
JTC-312-89	Bodmin Moor.	CGBG in road-cut.	SX 162 742
Gunnislake			
Granites			
JTC-200-89	Old Gunnislake Mine.	CGBG	SX 435 725
Mineralization			
JTC-197-89	Old Gunnislake Mine.	GBV in CGBG wallrock.	SX 435 725
Dartmoor			
Granites			
JTC-4-89	Haytor Mine.	Garnet-pyroxene-amphibole-bearing skarn.	SX 780 775
JTC-185-89	Merrivale Quarry.	CGBG	SX 545 745
JTC-187-89	Yellowmeade Farm Quarry.	CGBG	SX 565 735
JTC-188-89	Haytor Quarry.	CGBG	SX 755 774
JTC-189-89	Blockingstone Quarry.	CMG	SX 784 857
Mineralization			
JTC-212-89	East Vitafer Mine.	CGBG	SX 705 825
Hemerdon			
Mineralization			
JTC-318E-89	Hemerdon W-Mine.	Altered CGBG in drill core.	SX 570 585
JTC-319C-89	Hemerdon W-Mine.	GBV in drill core.	"

CGBG=Coarse-grained biotite granite, FGBG=Fine-grained biotite-granite, EBG=Equigranular biotite granite
CLMG=Coarse-grained Li-mica granite, FLMG=Fine-grained Li-mica granite, CMG=Coarse megacrystic granite,
FIG=Fluorite Granite, GBV=Greisen bordered vein.

* Samples from Darbyshire and Shepherd (1985), ** Collected by H. Bell, *** Collected by C. Smale